The International Journal of Advanced Manufacturing Technology (2020) 106:1869–1891
https://doi.org/10.1007/s00170-019-04732-9

ORIGINAL ARTICLE

Dynamic error of CNC machine tools: a state-of-the-art review

Dun Lyu[1] · Qing Liu[1] · Hui Liu[1] · Wanhua Zhao[1]

Received: 2 July 2019 / Accepted: 18 November 2019 / Published online: 13 December 2019

Abstract
The dynamic error of CNC machine tools, which often exceeds the quasi-static error at high-speed machining, becomes the main reason affecting the machining error of the sculptured surface parts. Although much research efforts have been dedicated to dynamic error, there is a lack of systematical summaries. In this review, firstly, the dynamic error is defined as the deviation of actual displacement of effector end of axis relative to reference displacement during feed motion. Secondly, according to the mechanical and control structure of the servo feed system, the dynamic error is divided into two components: dynamic error inside the servo loop (component 1) and dynamic error outside the servo loop (component 2). Based on the two components, the causes resulting in the dynamic error are analyzed from the points of view of the servo feed system itself and its input (setpoints). Thirdly, the basic strategies for reducing the dynamic error of individual axis, as well as for reducing the trajectory dynamic error by coordinating the dynamic error of individual axis, are summarized. Finally, the problems and future research directions on dynamic error are analyzed. It is concluded that resolving the contradiction between the setpoints and the servo feed system is still a great challenge for dynamic error in high-speed machining. To achieve high dynamic accuracy at high-speed machining, the control strategies on the dynamic error outside the servo loop should be further developed and integrated into dynamic error inside the servo loop-oriented control strategies. Meanwhile, the servo feed system itself and its input need to be investigated as a whole, so that the servo feed system of each axis can adapt to the differences and changes of the setpoints, and the differences in the servo dynamics of each axis can be considered in the setpoints.

Keywords Dynamic error · Servo dynamic error · Dynamic positioning error · Dynamic path error · Dynamic contour error · Machine tools

1 Introduction

Machine tool errors are errors in the position of the tool relative to the workpiece [1, 2], which are mainly caused by quasi-static error and dynamic error [1, 3].

Quasi-static error refers to the error when the machine tool does not move (spindle does not rotate or the worktable does not move) or the speed of motion is low, including geometric error and thermal error. Geometric error originates from manufacturing and assembling errors of parts. In addition, the deformation of structures caused by gravity causes the change of geometric error [4]. Thermal error is generated on account of the thermal expansion and distortion caused by the change of structure element and environment temperature [5]. There are some very nice reviews on the research progress of geometric error and thermal error in different periods. Sartori and Zhang [6] classified the methods for geometric measurement in direct and self-calibration methods, depending on the calibrated or uncalibrated standards. Ramesh et al. [7] summarized the sources and compensation methods of geometric error. Schwenke et al. [8] reviewed the direct measurement methods of geometric error and its compensation strategies. Ibaraki and Knapp [9] summarized the indirect measurement methods for internal error sources of three- and five-axis machine tools. Ramesh et al. [10] and Li et al. [5] reviewed the thermal error and its compensation methods of machine tool and spindle, respectively. Uriarte et al. [11] summarized measurement and compensation methods for geometric error and thermal error of large machine tools.

Dynamic errors have not been clearly defined so far and are generally considered to be related to feed motion [12]. The goal of dynamic error control is to achieve high trajectory

✉ Dun Lyu
dunnlu@xjtu.edu.cn

✉ Wanhua Zhao
whzhao@xjtu.edu.cn

[1] State Key Laboratory for Manufacturing Systems Engineering, Xi'an Jiaotong University, Xi'an 710054, China

accuracy. Schmitz et al. [13] carried out a case study, in which the grid plate encoder was employed to measure the trajectory errors of a circle–diamond–square tool path. They found out that the feed rate had effect on the trajectory errors. When the feed rate was increased from 150 to 8000 mm/min, the trajectory error of the circle–diamond–square tool path was increased from 6 to 11 μm, as shown in Fig. 1. Not only the feed rates, but also the acceleration/jerk [14] and the tool path curvature [15] have the effects on the dynamic errors, as well as the trajectory errors.

At high-speed machining of sculptured surface parts, the dynamic error is often greater than the quasi-static error, becoming the crucial factor to affect the machining error. After summarizing the development of machine tool feed drive from the transmission system, structural dynamic models, the control of rigid and flexible feed drives, etc., Altintas et al. [16] pointed out that there have been more than 10^5 rpm of spindles, which requires feed drives traveling over 5×10^4 mm/min with an acceleration of 10 g. Achieving the high dynamic accuracy is an ongoing hot topic and research challenge.

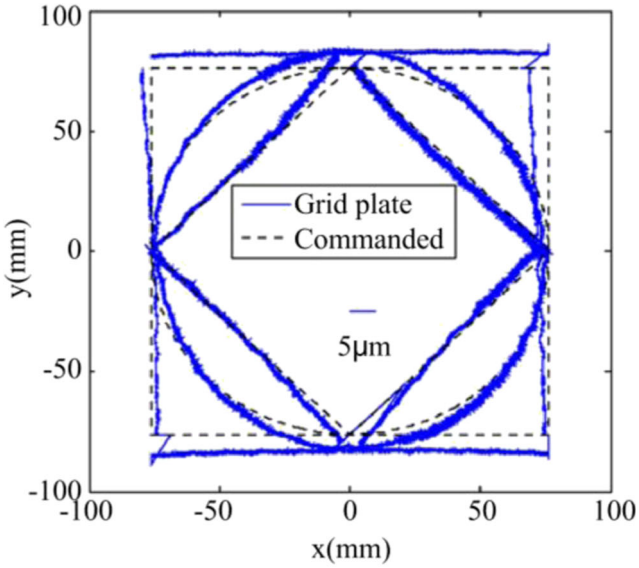

(a) 150mm/min

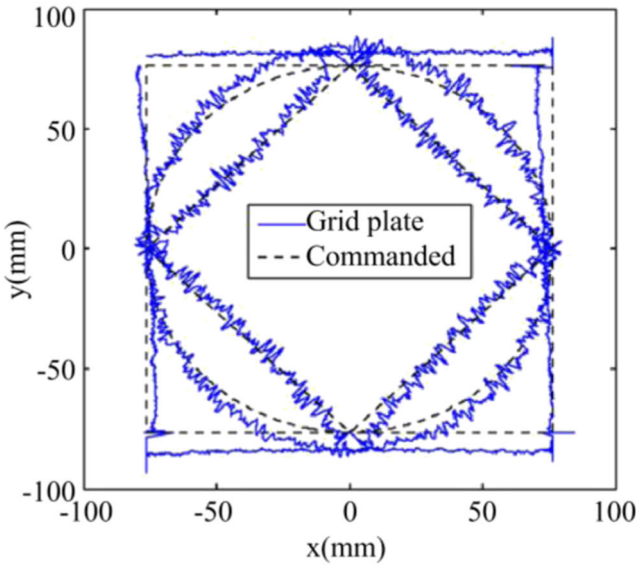

(b) 8000mm/min

Fig. 1 **a**, **b** Trajectory errors of the circle–diamond–square tool path measured by the grid plate encoder at two feed rates [13]

Although many research works related to the dynamic error have been published internationally, the complete and systematic summary on the dynamic error is still lacking. Some related reviews mainly summarized the research progress in each period around the individual axis tracking error control and the multi-axial tracking error coordinated control. Koren and Lo [17] summarized the feedback controller, feed forward controller, and cross-coupling controller early used in contour machining. Then, Koren [18] reviewed the servo control for individual axis, interpolators for coordinating the motion of several axes, and adaptive control for adjusting the cutting variables in real-time. Ramesh et al. [19] summarized the tracking error control systems and contour error control systems. Huo and Poo [1] summarized the control methods of trajectory tracking error, including individual axis tracking error control and multi-axis coordinated control. In multi-axis coordinated control, the cross-coupling controller and the methods of gain matching were mainly reviewed. Tang and Landers [20] summarized the research works of contour tracking control, including individual axis tracking control and multi-axis cross-coupling controller. In particular, the cross-coupling controller and its various improved methods were reviewed extensively. Jia et al. [15] carried out an extensive summary to the present state of the art of contour error control method research, including the contour error-oriented interpolation algorithm, individual axis tracking controllers, cross-coupling controllers, etc.

The above reviews revolve around the tracking error, involving the content of dynamic error partly, but the definition of dynamic error is still vague and the research framework is not clear. In this review, the definition of dynamic error is firstly given on the basis of summarizing the research of dynamic error in an all-round way. Secondly, based on the mechanical and control structure of the servo feed system, the dynamic error is divided into two components: the dynamic error inside the servo loop (component 1) and the dynamic error outside the servo loop (component 2). Then the causes of the two components of dynamic error are analyzed. Finally, the control methods of dynamic error are reviewed. In conclusion, the problems existing in the research of the dynamic error are analyzed and the future research directions are suggested. The contents of the existing reviews focused on the research progress of the tracking error in different periods are covered as component 1. Beyond that, the research progresses

on component 2 of the dynamic error are summarized. The contribution of this review is that the dynamic error of machine tool is clearly defined, and the research framework on the dynamic error is systematically presented.

It is noted that just the dynamic error related to feed motion is included. Although the disturbance, such as the harmonic force/torque of the motor [21–23], the cutting forces [24–26], the friction force [27–31], the pitch error of transmission [14], the transmission clearance [14, 32, 33], transmission harmonic component [34], etc., affect the dynamic error, the dynamic error caused by high feed rate, acceleration and jerk is often prominent in high-speed and high-precision machining. Therefore, the dynamic error caused by disturbance is not included.

2 Definition, components, and causes of dynamic error

2.1 Definition of dynamic error

Zhao et al. [34] systematically induced the classification of CNC machine tool errors, and then gave the definition of dynamic error, which is the deviation of the actual displacement of axis relative to the reference displacement, as shown in Fig. 2.

The mechanical and control structure of the *Y* axis of a five-axis machine tool is as shown in the upper half of Fig. 3 a. This axis is driven by a rotating motor and a ball screw. An encoder and a linear scale are used for closed loop control in velocity loop and position loop, respectively. The servo feed system of the *Y* axis has the longest mechanical series, including the mechanical transmission of the *Y* axis and the cascaded mechanical series of the *Z*, *A*, and *C* axes. The upper half of Fig. 3 b and c shows the mechanical and control structure of a ball screw feed system with semiclosed loop and the mechanical and control structure of a linear motor feed system.

It can be seen from the upper half of Fig. 3 that the actual displacement of axis is the actual displacement at the effector end of axis (e.g., the cutter or worktable). Thus, according to the definition put forward by Zhao [34], the dynamic error is the deviation of the actual displacement at the effector end of axis relative to the reference (setpoints) displacement in the feed motion.

2.2 Components and causes of dynamic error

It can be seen from the upper half of Fig. 3 that the deviation between the effector end displacement and the reference (setpoints) displacement can be divided into two components: the dynamic error inside the servo loop (component 1) and the dynamic error outside the servo loop (component 2).

2.2.1 Component 1: dynamic error inside the servo loop (tracking error)

Component 1 is the dynamic error inside the servo loop, which is usually called tracking error. For closed loop-controlled servo feed system, the tracking error is the deviation between the linear scale detecting displacement and the reference displacement, as shown in Fig. 3 a and c; for the semiclosed loop-controlled servo feed system, the tracking error is the deviation between the motor encoder detecting displacement and the reference displacement, as shown in Fig. 3 b.

The feed rate of setpoints at high-speed machining sculptured surface is usually not constant. The variable feed rate causes the tracking error to change along with it. Therefore, the tracking error is called as the dynamic error in some researches.

Slamani et al. [35] referred to the tracking error as servo error or servo dynamic error. Their research showed that the higher the feed rate is, the larger the servo dynamic error is. The servo dynamic error accounted for 80% of the volume error at a feed

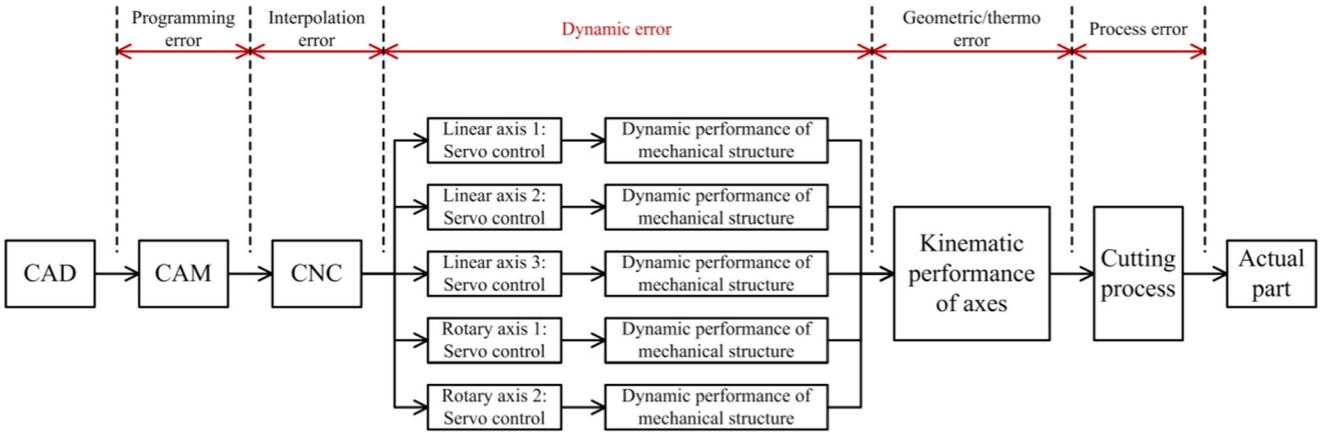

Fig. 2 Classification of CNC Machine tool errors induced by Zhao [34]

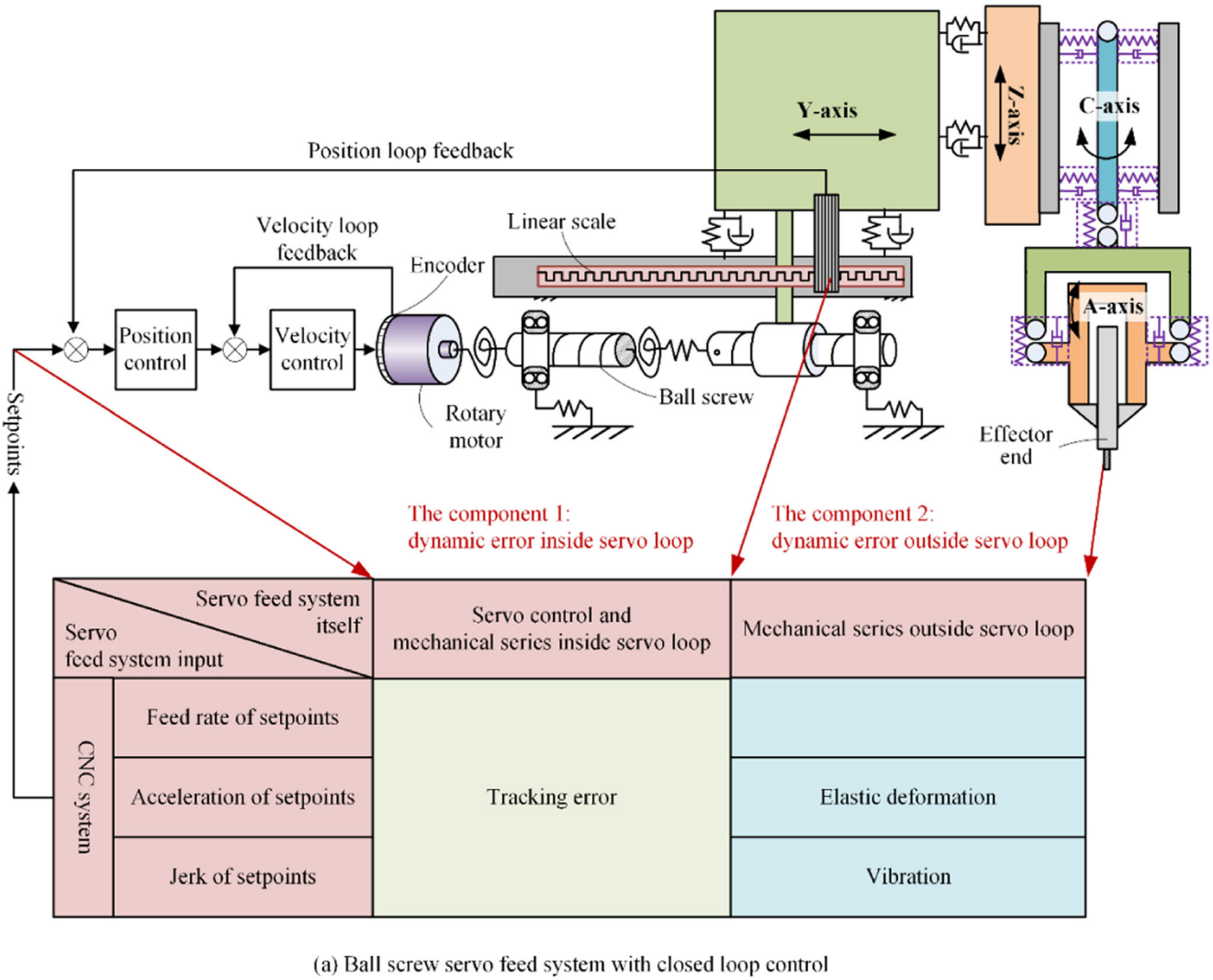

Fig. 3 **a**–**c** The definition, styles, and causes of dynamic error

rate of 10 m/min. Soon afterward, Slamani et al. [36] established the prediction model of servo dynamic error, which took the difference between output and input of the second-order system closed loop transfer function as the servo dynamic error. Chiu and Yao [27] referred to dynamic error as dynamic positioning error and stated that the dynamic position error was caused by the lack of bandwidth in the servo feed system. Zhao et al. [34] divided the tracking error into two states: steady state and transient state. The steady-state error is the position tracking error caused by time lag which is caused by acceleration and deceleration process and servo control. The transient error is the deviation between the reference displacement and the actual displacement caused by the adjustment and vibration excited by the sudden change of the setpoints. Zhong et al. [37] stated that the dynamic error is sensitive to tool trajectory and feed rate.

To sum up, the servo errors, servo dynamic errors, and dynamic positioning errors mentioned above are the deviation between the linear scale/encoder detecting displacement and the reference displacement. They are essentially the tracking errors which therefore belong to component 1 of dynamic error.

Component 1 of dynamic error originates from the phase lag of the servo system, but more importantly originates from the contradiction between the high setpoint bandwidth and the low servo bandwidth. When the setpoint bandwidth is larger than the servo bandwidth, the useful frequency component in setpoints which exceeds the servo bandwidth cannot be realized. The increase of the feed rate, acceleration, and jerk lead to the increase of the setpoint bandwidth, hence result in the increase of the tracking error. Servo bandwidth is related to mechanical dynamic characteristics. The mechanical modes both inside the servo loop and outside the servo loop may be the factors that limit the increase of servo bandwidth, as shown in lower half of Fig. 3.

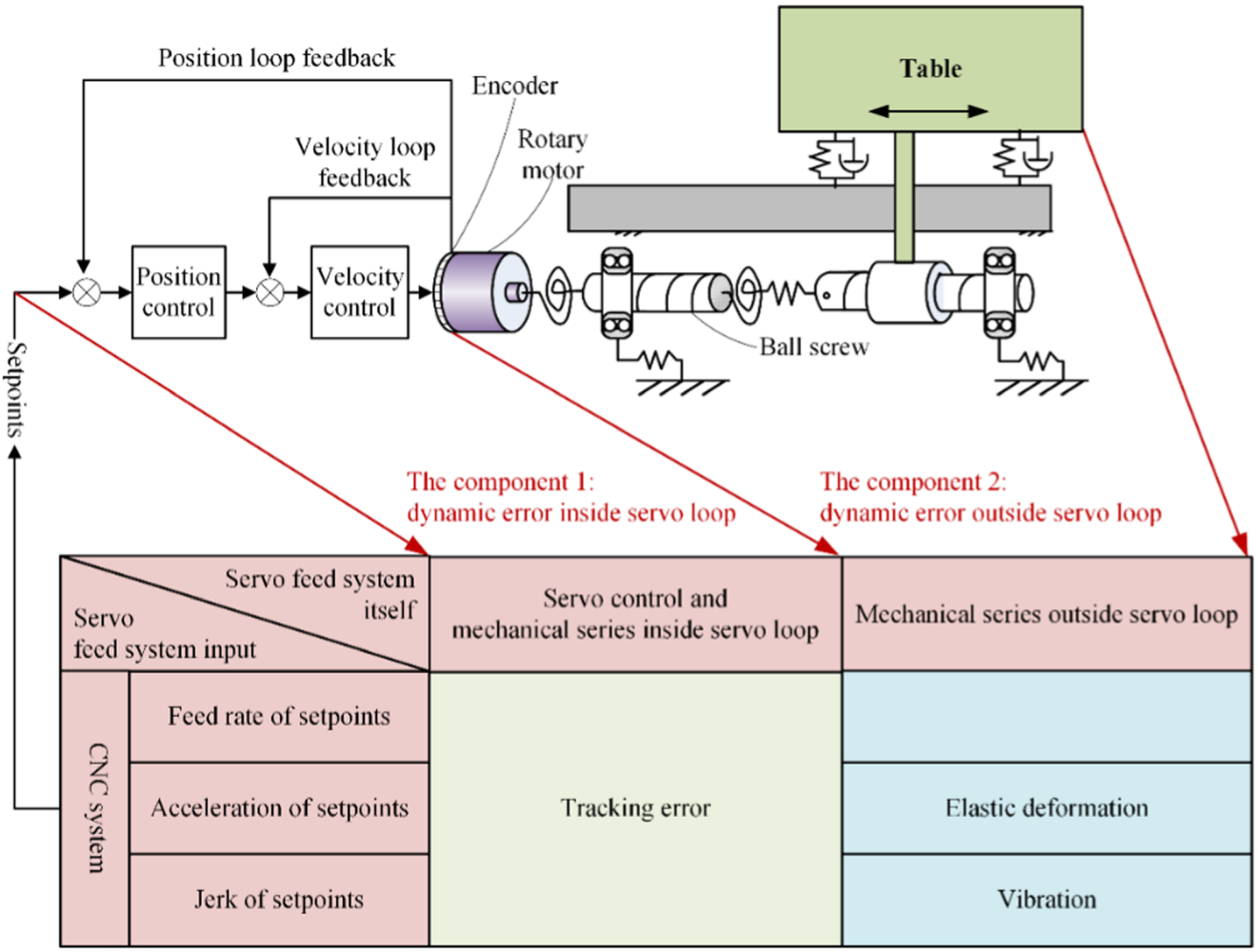

(b) Ball screw servo feed system with semi-closed loop control

Fig. 3 (continued)

2.2.2 Component 2: dynamic error outside the servo loop

Component 2 is the dynamic error outside the servo loop. For closed loop-controlled servo feed system, it is the deviation between the effector end displacement and the linear scale detecting displacement, as shown in Fig. 3 a and c; for the semiclosed loop-controlled servo feed system, it is the deviation between the effector end displacement and the motor encoder detecting displacement, as shown in Fig. 3 b.

In high-speed machining, the setpoints not only have high feed rate, but also have high acceleration. For example, for a given circular/corner path, when the path velocity is doubled, the required acceleration is increased by four times [38].

High acceleration causes high inertia force and, consequently, leads to the elastic deformation of mechanical series [39]. The jerk is the change rate of the acceleration which is regarded as the dynamic excitation [40], exciting the vibration of mechanical series. When the high acceleration and jerk act on the mechanical series outside the servo loop, it produces the deviation between the effector end and the closed loop/semiclosed loop detection point. This part of the error cannot be detected and controlled directly by the servo loop because the mechanical series is outside the servo loop. According to the difference of control type and mechanical structure, this kind of deviation can be classified into two cases: ball screw feed system with semiclosed loop control, as shown in Fig. 3 b and ball screw feed system and linear motor feed system with closed loop control, as shown in Fig. 3 a and c.

1. Ball screw feed system with semiclosed loop control

When the high acceleration and jerk of setpoints is input to the servo feed system, the mechanical transmission yields inertial force and inertial force excitation. For the ball screw servo feed system, the table is linked with the servo motor by the screw. Due to the finite stiffness, on the one hand, the

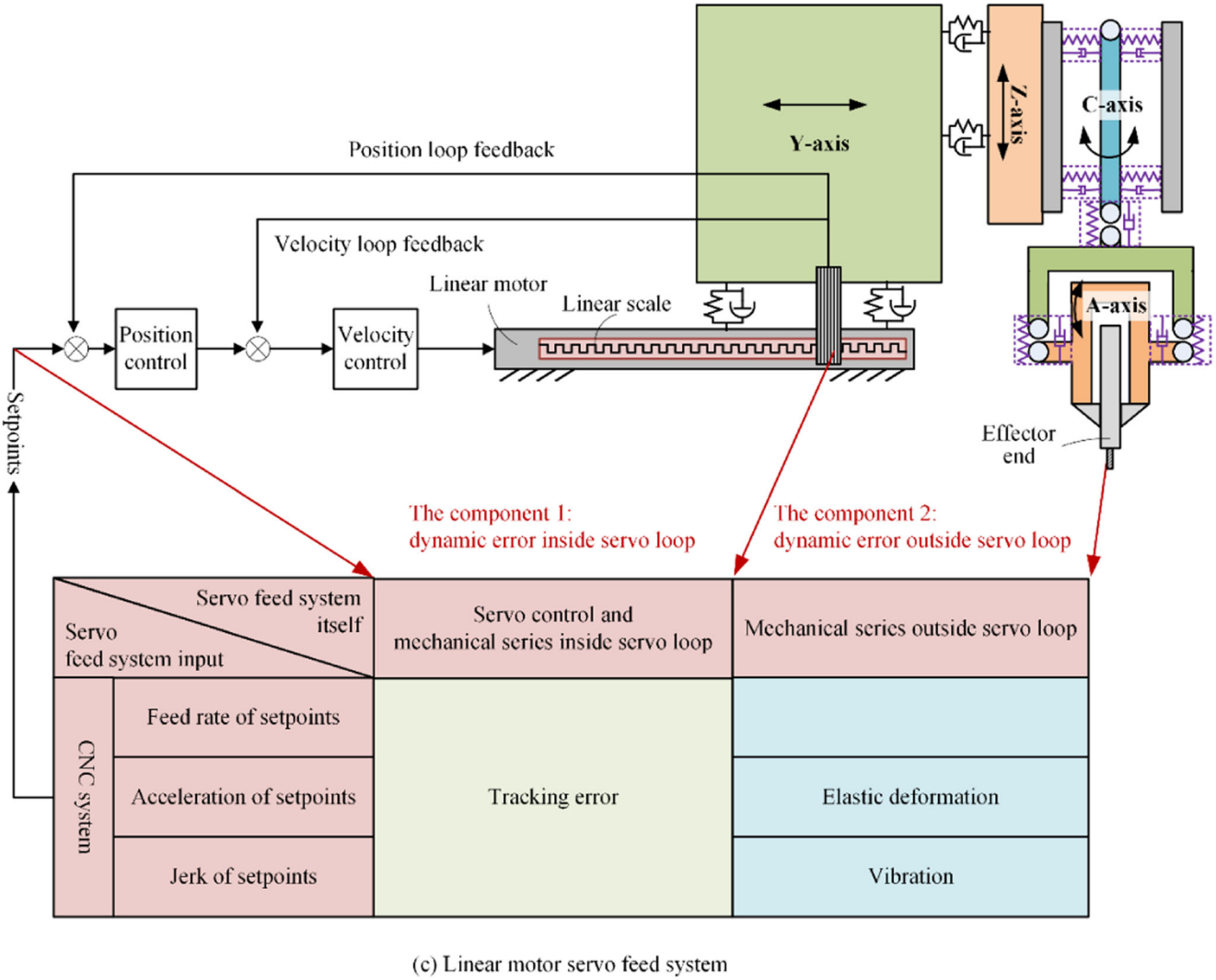

(c) Linear motor servo feed system

Fig. 3 (continued)

screw produces torsion [41–44] and elongation/compression [45] elastic deformations [46] under the action of inertia force, resulting in the difference between the motor and the worktable (this difference is also known as lost motion [43, 44] or loss of momentum [47]). On the other hand, under the action of inertial force excitation, the screw produces vibration. Therefore, the dynamic error includes elastic deformation and vibration.

In semiclosed loop control, the servo system uses the signal of the encoder attached to the motor as the feedback signal, which can only control the error at the motor, but cannot correct the error at the worktable's position caused by the elastic deformation of the screw [42].

In closed loop control, the servo system uses the signal of linear scale as the feedback signal, which can significantly reduce the elastic deformation of the screw [45, 46]. However, the vibration caused by inertial force excitation still exists. This kind of vibration is an important factor to limit the improvement of the servo bandwidth, which affects component 1 of dynamic error.

To sum up, for the ball screw feed system with semiclosed loop control, this component of dynamic error includes elastic deformation and vibration of mechanical transmission which originates from the acceleration and jerk of setpoints, respectively.

2. Ball screw feed system and linear motor feed system with closed loop control

For the multi-axis machine tool with series structure, because of the limitation of the structure, the feedback elements in some axes, such as linear scales, cannot be installed close to the end of effector, even if the closed loop control is adopted, which results in many mechanical series outside the servo loop. Whether it is the ball screw feed system shown by Fig. 3 a or the linear motor feed system shown by Fig. 3 c, the feedback position is far from the effector end.

Under the action of the acceleration of setpoints, the mechanical series outside the servo loop produces the inertial force which has usually an offset from the driving force (the driving force and the inertial force are not on the same line). The offset further produces the moment of inertial force [48] which causes the elastic deformation of the mechanical series [38, 49–51], as shown in Fig. 4. The amplitude of the elastic deformation is linearly correlated with the acceleration and offset distance [53].

Under the action of jerk of setpoints, the eigenmodes of mechanical series outside the servo loop can be excited [51], which lead to the vibration of mechanical series outside the servo loop [38, 49, 50]. In order to eliminate the vibration, it is necessary to limit the jerk [11, 54].

The elastic deformation and vibration of the mechanical series outside the servo loop cannot be controlled by the closed loop [11, 54–57]. It can lead to surface quality defects in high-speed milling of corners, sharp edges, and S-shaped curves, which are typical technological features with significant elastic deformation and vibration. Large and heavy machine tools usually produce a larger elastic deformation and vibration at a given acceleration. Columnar and portal machine tools are more likely to produce elastic deformation and vibration than C-shape and box-in-box machine tools [52].

The elastic deformation and vibration of the mechanical series outside the servo loop, directly relating to the inertial force and inertial force excitation [58], are widely regarded as the dynamic error. However, the definition of the dynamic error is different according to different concerns. Bringmann and Maglie [51] defined the dynamic error as dynamic path error, which is the relative dynamic displacement between the tool and workpiece at the tool tip point. By using the R-test method, they measured the error of the dynamic trajectory in three translational degrees of freedom, in which one was the feed direction and the other two were perpendicular to the feed direction. ISO 230-8 defined the dynamic displacement at the tool tip as inertial cross-talk [59]. Andolfatto et al. [60] defined the additional error as the dynamic geometric error, which is produced in high feed rate, as shown in Fig. 5. This error is from the elastic deformation of the mechanical series with the action of inertial force during the acceleration process. They also found that the dynamic geometric error is related to the feed rate, and also positively correlated with the feed acceleration. In addition, the dynamic geometric error is obvious at the sharp corner. Kono et al. [61] defined the error between the tool tip and control detector position as dynamic mechanical error. They pointed out that the error is mainly caused by the dynamic response of the mechanical system.

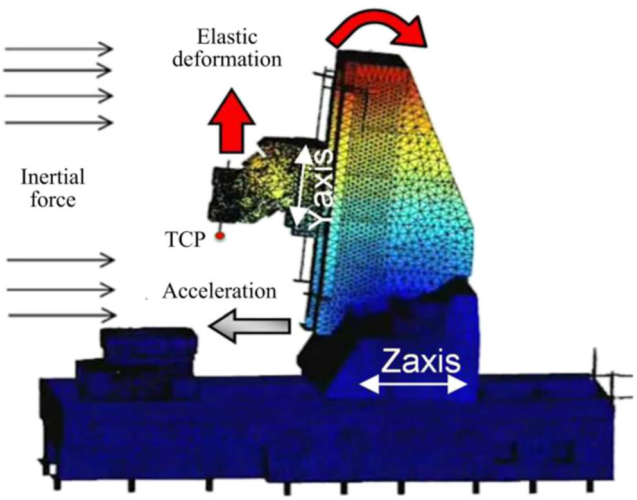

Fig. 4 Elastic deformation of mechanical series outside the servo loop caused by inertial force [52]

To sum up, the dynamic geometric error, the dynamic trajectory error, and the dynamic mechanical error mentioned above are essentially the elastic deformation and vibration of mechanical series outside the servo loop. Therefore, these errors belong to component 2 of dynamic error which originates from the acceleration and jerk of setpoints, including the elastic deformation and vibration of mechanical series outside the servo loop. The acceleration produces the inertial force and, hence, causes the elastic deformation, while jerk as an excitation arouses the vibration.

The dynamic error consists of inside servo loop dynamic error and outside servo loop dynamic error. In Section 2, the concepts mentioned in the literature (as shown in Table 1) such as the servo dynamic error, dynamic position error, dynamic geometric error, dynamic trajectory error, etc. are essentially one component of dynamic error.

The dynamic error is the deviation between the actual displacement of the axis and the reference displacement and is the superposition of the dynamic errors in component 1 and component 2. The component dominating of dynamic error is related to many factors, including mechanical structure, control system, setpoints, tool path, etc. But in general, the dominating component depends on the servo feed system itself and its input (setpoints) [62]. Consequently, this review induces the components and the causes of dynamic error from the two dimensions: the servo feed system itself and its input, as shown in the lower half of Fig. 3.

The requirement of CNC machine tools is to coordinate the movement of the axes to trace a predetermined trajectory of the tool relative to the workpiece accurately [63]. If the dynamic error of all the individual axes can be minimized to a very small value, the trajectory accuracy can be realized. Therefore, Sections 3 and 4 will summarize the research works of minimizing dynamic error from the aspects of the servo feed system itself and input, respectively. However, the dynamic error of individual axis is often difficult to be completely eliminated. In this case, the trajectory accuracy can only be ensured by coordinating the dynamic error of all the individual axes. Therefore, in

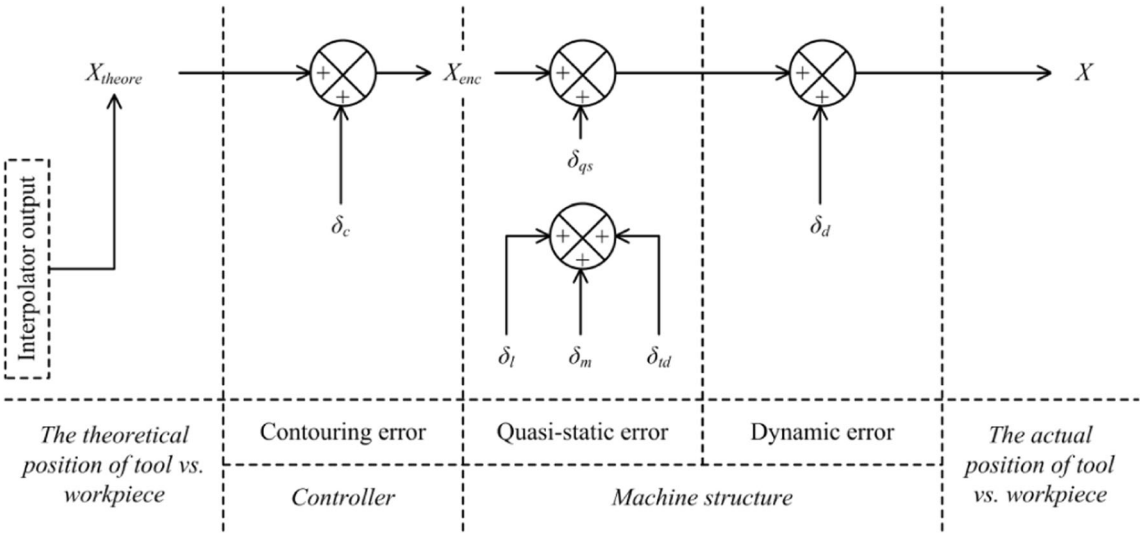

Fig. 5 Servo error, quasi-static error, and dynamic error defined by Andolfatto et al. [60]

Section 5, some research works on coordinated control will be summarized.

3 Minimizing the dynamic error from the aspects of the servo feed system itself

3.1 Improvement of the phase– and amplitude–frequency characteristics for minimizing the dynamic error inside the servo loop (component 1)

3.1.1 Improvement of phase–frequency characteristic by reducing phase lag

The phase lag causes the time delay between the actual displacement and the reference displacement. The representative solving method for the phase lag is the zero phase error tracking controller (ZPETC) proposed by Tomizuka [64], as shown in Fig. 6. ZPETC takes the inverse of the servo feed system model as the feed forward transfer function on the basis of elimination for the unstable poles, making the phase difference in the steady state to be 0 in the frequency domain and the static (frequency is 0) gain to be 1. Funahashi and Yamada [65] improved the phenomenon of ZPETC gain decreasing with the increase of frequency by means of feed forward gain filter compensator. ZPETC can only be used in a low-frequency range, but cannot implement effective control in a high-frequency range (e.g., circular follow process) [66].

ZPETC depends on the accuracy of the system model [66]. The variation of the system parameters and disturbance can result in the failure of the controller. To enhance antiparameter variation and antidisturbance ability, ZPETC needs to combine with friction, reverse gap and trajectory error

Table 1 Literatures about the definition, components, and causes of dynamic error

Dynamic error	Literatures
Component 1 and its causes	Chiu and Yao [27] Zhao et al. [34] Slamani et al. [35, 36] Zhong et al. [37]
Component 2 and its causes	Heisel and Gringel [38] Kono et al. [39] Barre et al. [40] Lim et al. [41] Zhu and Fujimoto [42] Sugie et al. [43, 44] Kamalzadeh et al. [45] Huang et al. [46] Wu et al. [47] Dong et al. [48] Weekers [49] Ahmadian et al. [50] Bringmann and Maglie [51] Knapp and Weikert [53] Parenti et al. [52] Ansoategui et al. [54] Thoma et al. [55] Nguyen et al. [56] Zatarain et al. [57] Mu and Ngoi [58] ISO 230-8 [59] Andolfatto et al. [60] Kono et al. [61]

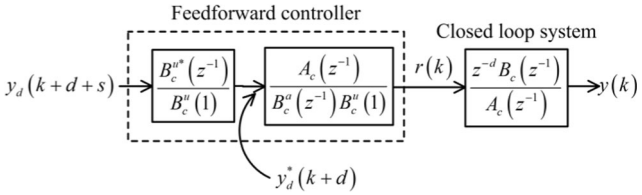

Fig. 6 Zero phase error tracking controller (ZPETC) developed by Tomizuka [64]

compensation [67], disturbance observer [68], and robust controller [69].

3.1.2 Improvement of amplitude–frequency characteristic by increasing bandwidth

With the development of high-speed machining, the feed rate has been increasing. The high feed rate leads to the high-frequency setpoint bandwidth exceeding the servo bandwidth, which is the main factor causing the tracking error [70]. Therefore, control methods to increase servo bandwidth have been attracting much attention.

The servo bandwidth of ball screw servo feed systems can only reach 30 Hz [16] to 50 Hz [62]. When the feed rate reaches 40 m/min and the acceleration reaches 2 g, the servo bandwidth must reach 100 Hz for effective control of the tracking error in the machining of aeronautical structural parts [70].

For the ball screw servo feed system, the axial and torsional vibration modes of the screw limit the servo bandwidth. Chen and Tlusty [71] compensated the two torsional vibration modes by zero pole cancelation. They increased the servo bandwidth to 100 Hz. Erkorkmaz and Kamalzadeh used adaptive sliding mode controller to suppress the first-order axial vibration mode [72] and the notch filters to suppress the first- and second-order torsional vibration modes [73], which increased the servo bandwidth to above 200 Hz, as shown in Fig. 7.

In addition to using filters to increase servo bandwidth, researchers have been exploring advanced control strategies. Altintas et al. [74] developed an adaptive sliding mode controller to increase the servo bandwidth of the ball screw servo feed system to above 60 Hz. Then Okwudire and Altintas [75] proposed adaptive disturbance discrete-time sliding mode controller to increase servo bandwidth above 200 Hz. Pritschow and Croon [76] placed low stiffness bearings and large dampers in servo feed systems to increase the servo bandwidth by six times. Verl and Frey [77] proposed a semi-active damping control method using a friction-based actuator to selectively suppress vibrations, which increased the bandwidth of the position loop by 100%. Moreover, the jerk was doubled under the same tracking error (Fig. 8).

Sun et al. [78] proposed an additional table speed control loop based on the traditional P-PI cascade control structure to increase the bandwidth of the position loop, as shown in Fig. 9. Based on this control structure, the speed difference between the motor and the table was used as the mechanical vibration to the speed controller to increase the position loop bandwidth by 80% [79]. Since then, they [80] further improved this method by setting the speed loop as a small gain proportional control and setting the position loop as PD control, as well as adding the disturbance observer, which increased the bandwidth of the position loop by 200% and decrease the tracking error by 70%.

Sencer and Dumanli [81] proposed an optimal controller using the load side feedback signal. With their controller, the bandwidth was increased to more than 300 Hz at a feed rate of 48 m/min and acceleration of 2.5 g, and the tracking error was reduced to 40 μm without feed forward compensation. Liu et al. [82] analyzed the reason of bandwidth limitation from the point of view of noncollocated control. They stated that the position feedback point and driving point of the motor were noncollocated under closed loop control. The noncollocated control caused the nonphase vibration and instability and, hence, resulted in the limitation of the bandwidth. They used the peak filter control to adjust the nonphase vibration to the in-phase vibration, as shown in Fig. 10. As a result, the gain of the speed control loop was increased, and the negative effect of noncollocated control on the position control loop was eliminated. Dumanli and Sencer [83] presented an optimal noncollocated pole placement control technique for flexible ball screw drives, in which a kinematic state observer was

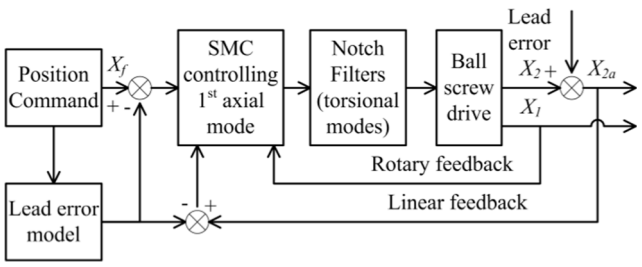

Fig. 7 Sliding mode and notch filter controller proposed by Erkorkmaz and Kamalzadeh [72]

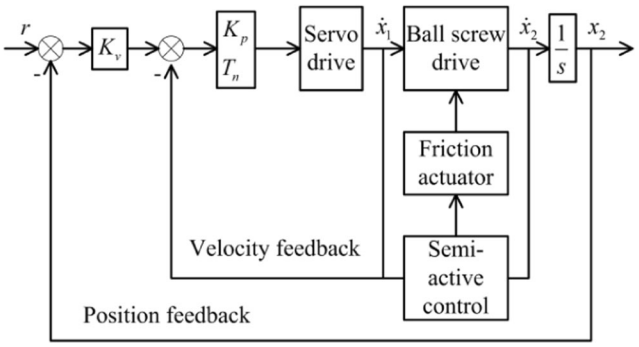

Fig. 8 Control structure for the feed drive with semi-active damping proposed by Verl and Frey [77]

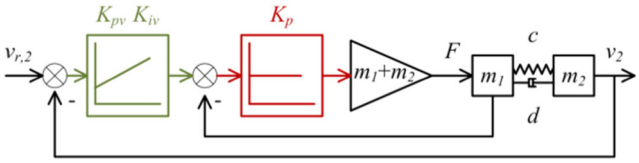

Fig. 9 P-PI control structure with an additional table speed loop developed by Sun et al. [78]

developed that fused accelerometer and encoder measurements together to enable noncollocated control on ball screw drives.

In order to suppress the vibration, additional active damping needs to be added in the closed loop. Fanuc proposed a vibration damping control function which could suppress the vibration by inputting the difference value of encoder and linear scale to the torque command [84]. Heidenhain developed an active vibration damping option which could reduce the low-frequency vibration from the mechanical transmission as well as the whole machine [85].

Increasing the bandwidth of the servo system can reduce the tracking error, but may result in a larger sensitivity to higher-frequency disturbances. In order to balance tradeoffs between low-frequency tracking properties and high-frequency disturbance sensitivity, van Loon et al. [86] proposed a bandwidth-on-demand variable gain control strategy, as shown in Fig. 11, which is able to adjust controller gain online to achieve bandwidth adjustment according to the variation of feed rate.

3.2 Control methods for dynamic error outside the control loop (component 2)

3.2.1 The compensation of screw elastic deformation of ball screw servo feed system with semiclosed loop control

Component 2 of dynamic error of a ball screw feed system with semiclosed control is as shown in Fig. 3 b.

In order to reduce the elastic deformation of the ball screw under the semiclosed loop control, Lim et al. [41] proposed a torsional displacement compensation method including an algorithm of torsional displacement feedback and an estimation method of torsional displacement. Kamalzadeh et al. [45] established the relationship between elastic deformation and inertia force for estimating the elastic deformation. The estimated elastic deformation was compensated by offsetting the setpoints. Huang et al. [46] derived the expressions of inertial force, viscous forces, and elastic deformation in the feed motion. On this basis, they developed an interpolation algorithm which could generate the modified setpoints to compensate the elastic deformation, as shown in Fig. 12.

3.2.2 The control of dynamic error outside the servo loop of the servo feed system with closed loop control

For a ball screw feed system and a linear motor feed system with closed loop control, component 2 of dynamic error is as shown in Fig. 3 a and c.

The control for component 2 of dynamic error should be carried out on the basis of online estimation or offline measurement. The model-based control, actual position estimation of effector end through external sensors, and measurement are the main methods employed in the current research.

In terms of model-based control, Wang et al. [87] established a dynamic model of three-axis gantry machine tool considering inertial force and analyzed the effect of coupling force on tool tip point deviation during acceleration and deceleration. Parenti et al. [52] decomposed the dynamic error at high acceleration feed into static component proportional to instantaneous acceleration and dynamic component coming from the vibration excited by jerk. On this basis, a model-based compensation scheme was proposed, as shown in Fig. 13. Matsubara et al. [88] proposed a model reference feedward controller.

In terms of actual position estimation of effector end through external sensors, Zatarain et al. [57] employed an acceleration sensor installed near the tool to predict the position of tool center point. They used the predicted position as the position feedback instead of the position read by the linear scale. Denkena et al. [89] integrated Kalman filter into the cascaded control of the servo feed system based on the mechanical rigid body model, as shown in Fig. 14. Receiving the tool vibration data measured by laser vibrometer and linear scale data, the Kalman filter could predict the position and velocity at tool tip point and sent it as feedback signals.

In terms of measurement, Weikert [90] put forward the R-test measuring device, which was used to measure the error of

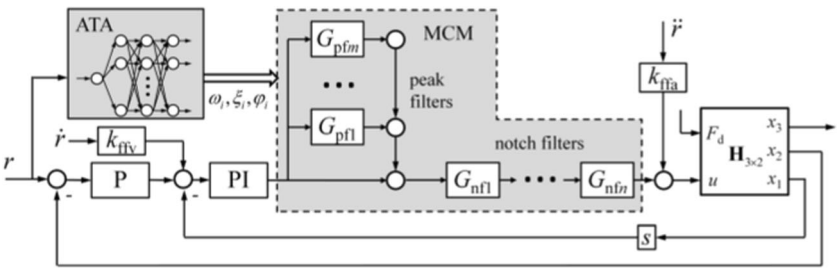

Fig. 10 An intelligent noncollocated control strategy for ball screw feed drives with dynamic variations proposed by Liu et al. [82]

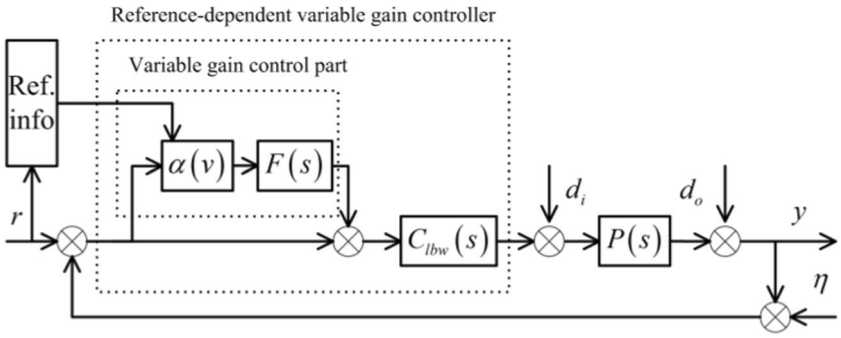

Fig. 11 The bandwidth-on-demand variable gain control strategy proposed by van Loon et al. [86]

the five-axis machine tool. Based on this measuring device, as shown in Fig. 15, the measurement and evaluation method of dynamic 3D trajectory error of the five-axis machine tool at the tool tip point was investigated by Bringmann and Maglie [51]. Thoma et al. [55] also used the R-test to measure the pitching errors caused by inertial force. They classified the pitching error into inertial cross-talk and inertial in-talk. The inertial in-talk is the position deviation along the feed direction, while the inertial cross-talk is the straightness deviation along the direction perpendicular to the feed direction. Steinlin et al. [91] compensated cross-talk error offline based on the actual measurement data. Keck et al. [92] proposed an active control system including a model-based compensation system for dynamic errors to increase acceleration. An optical sensor permitting the direct measurement of the actual tool center point position was used for system identification of the required dynamic model.

4 Minimizing the dynamic error from the aspects of the servo feed system input (setpoints)

The setpoints, as the inputs of the servo feed drive system, are generated by interpolation of the CNC system. The setpoint interpolation is a process in which the geometric tool path is transformed into the temporal motion setpoints of machine tool axes under the multiconstraints of geometric precision, kinematic constraints of axes, smoothness motion profile, etc. Firstly, the setpoints must meet the requirements of tool path geometric accuracy [93]. Secondly, the setpoints should make full use of the kinematic constraints of machine tool axes to increase the machining efficiency [94]. Finally, the setpoint profile (feed rate/accelerate/jerk profile) should be smooth, so that it is easy to achieve high tracking accuracy and free of vibration [95].

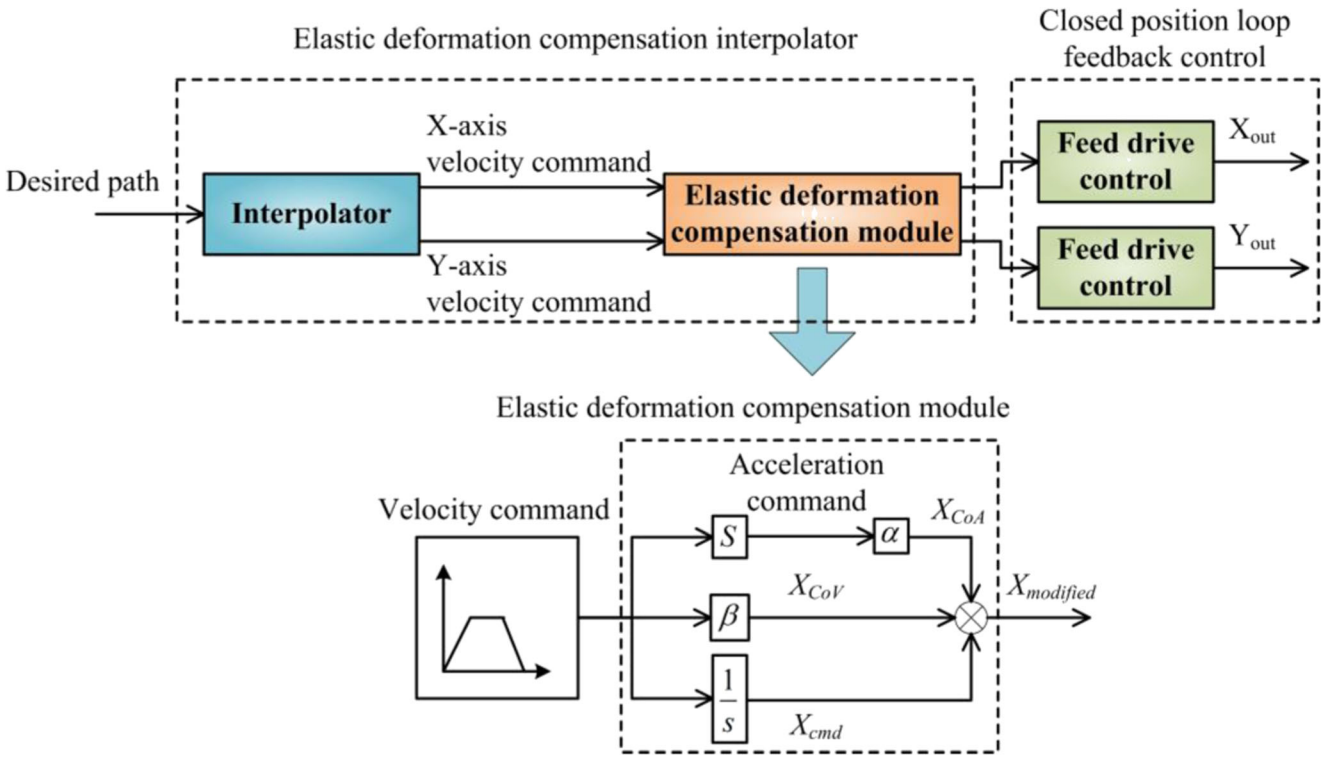

Fig. 12 The elastic deformation compensation interpolation (EDCI) module proposed by Huang et al. [46]

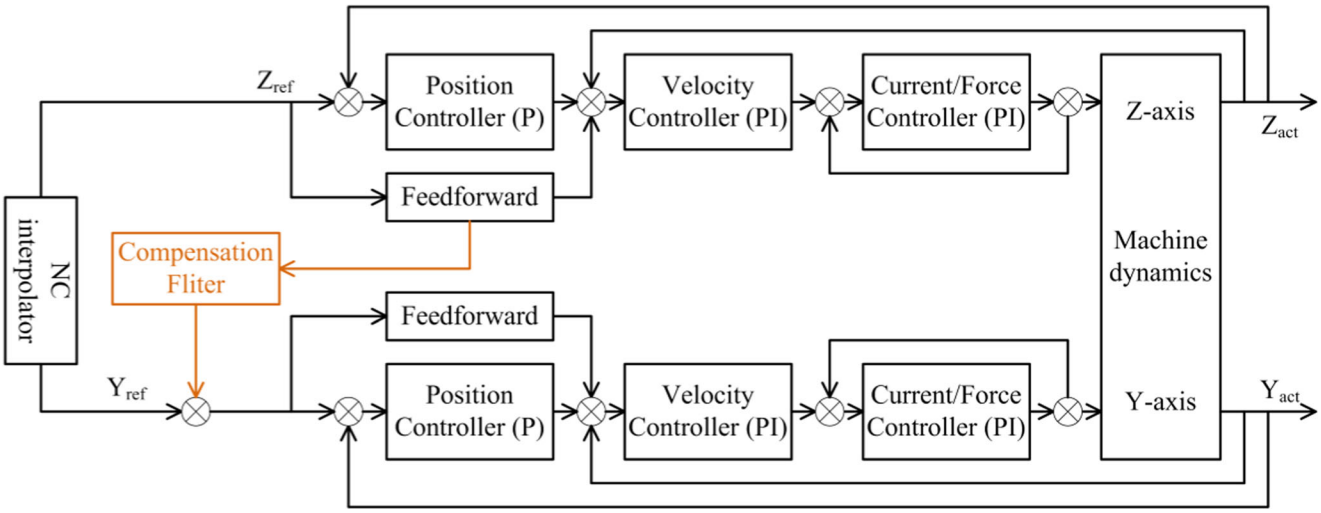

Fig. 13 Model-based compensation scheme proposed by Parenti et al. [52]

Among the many constraints in the interpolation process, the smoothness of setpoints is the main factor that affects the dynamic error. The smoothness of setpoints requires the smoothness of the feed rate, acceleration, and jerk profile. If the feed rate profile is not smooth, the setpoint bandwidth increases, and the servo system is not able to follow the useful frequency component of the setpoints beyond the servo bandwidth, resulting in the tracking error. If the acceleration and jerk profiles are not smooth, the setpoints contain more frequency components, which can easily excite the vibration of mechanical structure.

Many factors, such as the programmed feed rate, limitation of acceleration and jerk, and the curvature of the tool path and so on, affect the dynamic error through the smoothness of the feed rate, acceleration, and jerk profile. Generally, the smoothness of setpoints is related to the CAM and CNC. In the CAM, the generated tool path itself should be smooth. In the CNC, the generated feed rate profile should be smooth.

4.1 Tool path smoothing

Some CAM systems can generate NC codes in parametric curve formats which are C^2 continuous. Directly interpolating these parameter curves, CNC systems can generate smooth setpoints [96, 97]. Interpolation algorithms on parametric curves, such as quintic spline [98], polynomial curve [99], hermit curve, B-spline curve [100], Bezier curve [101], Akima curve [102], NURBS-based parametric curves [103], etc., have been widely investigated, in which NURBS-based parametric curves are paid more attention [104, 105]. The interpolation for parametric curves is essentially an optimization problem, and it is extremely difficult to get the time-optimal solution. In order to solve this problem, Zhong et al. [106] developed a real-time interpolator for parametric curves, in which the look-ahead length was dynamically adjusted to minimize the computation load. Moreover, the interpolator took into

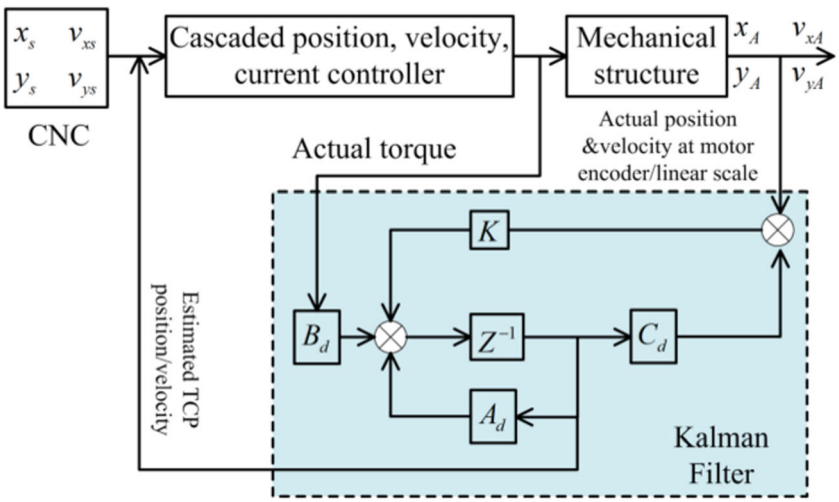

Fig. 14 Integration of the Kalman filter in the cascaded control proposed by Denkena et al. [89]

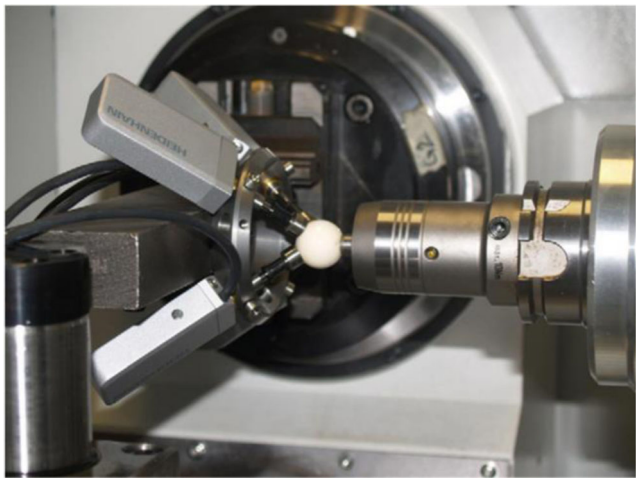

Fig. 15 The measurement of the accuracy of dynamic trajectory using the R-test [51]

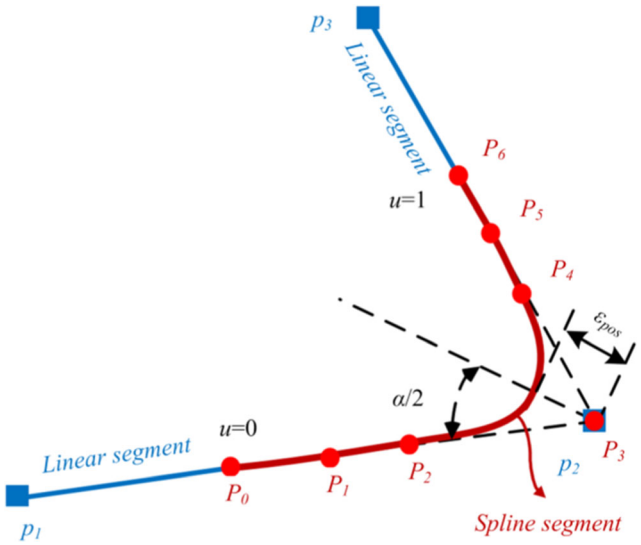

Fig. 16 Smoothing sharp corner with quintic B-spline [110]

consideration of constraints from machine dynamics and contour error while maintaining the feed rate as high as possible.

At present, most CAM systems cannot output parametric curve tool paths, but can only output polygonal tool paths composed of consecutive line segments. Polygonal tool paths are only continuous in position, but its tangent and curvature are discontinuous. In the corners of consecutive line segments, smooth setpoints cannot be interpolated. The motion must stop at the corner shallowly; otherwise, the driver will violate the maximum acceleration and jerk limitation.

The methods of generating smooth motion without stopping along the polygonal tool path are global smoothing [107] and local corner smoothing [108] of the tool path by parametric curves.

Global smoothing employs parametric curves to approximate the discrete reference points in tool paths, which can be carried out in the workpiece coordinate system or in the machine tool coordinate system [108, 109].

Local smoothing employs transition parameter curves to blend the corners in consecutive line segments locally, as shown in Fig. 16. The basic arcs, quadratic curves, quintic curves [110–112], cubic B-splines [113], PH curves [108, 114], etc. are selected as transition parameter curves, in which cubic B-splines have the lowest degree to achieve G^2 continuity. The transition curves overlap with each other when the two adjacent lines are not long enough. In order to avoid this problem, Tajima and Sencer [115] developed a method of interpolating the velocity and acceleration of the axis near the corner directly.

The smoothness of the five-axis tool path is more complex than that of the two-/three-axis tool path, which requires not only the smoothing of the tool tip path, but also the tool orientation path. Beudaert et al. [116] used the dual spline approach to smooth the five-axis tool path. One spline was used to smooth the tool tip path and the other one was used to smooth the tool orientation path. Tulsyan and Altintas [110] adopted the quintic and heptic micro splines, respectively, to smooth the tool tip path and the tool orientation path. Shi et al. [108] used a pair of quintic PH curves to round the corners of the tool tip path and the tool orientation path. Tajima and Sencer [117] proposed an online interpolation of five-axis machining tool path in workpiece coordinates. TCP motion was interpolated and locally blended in Cartesian coordinates by finite impulse response filtering of axial velocity components, and tool orientation was blended directly in spherical coordinates.

4.2 Setpoint profile smoothing

Setpoint profile smoothing is usually called as feed rate planning or feed rate interpolation, which is a key task of the CNC system to generate a setpoint for each axis. Feed rate planning is a multiconstraints problem which needs to take into account restrictions of geometric errors, kinematic parameters, smoothness of setpoint profiles, etc. [118].

Firstly, the feed rate planning needs to consider the geometric error which is influenced by both the feed rate and the curvature of the tool path. Under the same tool path curvature, the larger the feed rate is, the greater the geometric error is. Therefore, for the tool path with sharp curvature change, the feed rate should be adjusted with the curvature change in order to improve the machining efficiency under the premise of satisfying the geometric error [119].

The traditional constant increment interpolators [100], updating the parameter u uniformly with a constant increment, can cause significant feed rate fluctuation. The constant feed rate interpolators, using Taylor's series to calculate the parameter u, can keep the constant feed rate [120]. However, this

method causes very large chord errors on the break points with just C^0 continuity and on the critical points with high curvature [121]. The adaptive feed rate interpolators can adaptively adjust the feed rate according to the relation among feed rate, geometric error, and curvature [122, 123]. Jia et al. [124] defined a large curvature region with the allowable feed rate less than the programmed value as the feed rate-sensitive region. Different constant feed rates were assigned in different sensitive regions to further improve the smoothness of feed rate profile.

Secondly, the feed rate planning should avoid the feed rate, acceleration, and jerk of setpoints beyond the kinematic constraints of each axis [125, 126]. In addition, the kinematical ability of the machine tool can be making the best use to improve the machining efficiency by the look-ahead scheme [109, 127, 128]. In the consecutive line segment interpolation, the look-ahead scheme realizes the maximum feed rate under the restriction of the machine tool kinematic parameters through the pre-read several blocks of NC codes [129]. It can not only overcome the frequent start/stop motions, but also improve the machining efficiency. Furthermore, the look-ahead scheme can detect the position and adjust the feed rate at the sharp corner in the consecutive line segment interpolation, as well as the parametric curve interpolation [107, 130].

Finally, the feed rate planning should make the setpoint profiles as smooth as possible. The acceleration-limited trapezoidal-shape feed rate planning can just generate the continuous feed rate profile [131]. The jerk-limited S-shape feed rate planning can generate the continuous feed rate and acceleration profiles [98, 113, 121, 129, 132], while the jerk continuous (such as trigonometric) feed rate planning can realize the continuous feed rate, acceleration, and even jerk profiles [133]. Altintas et al. [16] compared the spectrum of acceleration profile generated by trapezoidal feed rate planning (velocity continuity), trapezoidal acceleration feed rate planning (acceleration continuity), and cubic acceleration feed rate planning (jerk continuity), as shown in Fig. 17. The last one has the least amount of acceleration amplitude at high frequencies.

In high-speed machining, cut feed rates greater than 60 m/min and accelerations higher than 2 g have been used. In such high feed rates and accelerations, even a small discontinuity in curvature or in tangency can result in jerk spikes and, consequently, in machine vibrations [134]. Therefore, eliminating the vibrations excited by jerk has been paid intensifying attention in the past few years. Shahzadeh et al. [134] proposed a path smoothing method using biclothoid fillets. The fillet fitting was not limited to line to line transitions. It can be fitted between two arcs or a line and arc as well. Tajima et al. [135] used a chain of FIR filters to generate the acceleration and jerk continuous feed rate. Sencer and Tajima [136] presented a feed rate planning technique, which had the capability to avoid excitation of inertial vibrations. In their method, the time-stamped acceleration profile of the feed profile was defined as a ninth-order polynomial. The polynomial coefficients were solved through an optimization procedure where the objective function penalized total frequency energy in a desired frequency band. As a result, generated reference acceleration commands did not contain any excitation near the vibration modes. Tajima and Sencer [115] proposed a real-time interpolation algorithm to generate continuous rapid feed motion along short segmented linear tool paths by smoothing local and adjacent corners that were within close vicinity to generate a global jerk-limited high-speed motion trajectory. Sencer et al. [137] presented a technique to generate reference trajectories with optimal frequency spectra to avoid machine tool vibrations during linear point-to-point and spline interpolation. In their method, reference acceleration profiles were generated so that their spectral energy was attenuated around vibration mode(s) of the machine.

The approaches of feed rate planning are generally divided into two categories. The first approach uses modeled process constraints in order to constrain velocities, accelerations, and jerks during a preprocessing operation. The second approach employs measured process parameters for limiting axis accelerations and velocities by adjusting the overall feed rate in real-time. Mansour and Seethaler [138] developed an algorithm that allowed combining the measured and modeled process constraints.

4.3 Setpoint filtering and shaping

In order to further eliminate the high-frequency components in the setpoints after tool path and feed rate smoothing, prefiltering and shaping techniques can be used to remove the frequency component which can excite the mechanical modes.

Weck and Ye [95] set a low-pass filter before ZPETC to filter out the high-frequency components, so that the control performance of ZPETC for corner tracking was improved. Liu et al. [130] used the notch filtering to eliminate the mechanical natural frequency component contained in the setpoints in NURBS parameter curve interpolation, as shown in Fig. 18.

Singer and Seering [139] and Dietmair and Verl [140] investigated input shaping methods for avoiding the structural vibration. Altintas and Khoshdarregi [141] shaped the setpoints to avoid the excitation of the targeted structural frequencies. Jones and Ulsoy [142] designed the feedforward filter to shape the setpoints and reduced the peak-to-peak vibration magnitude by 50%. Okwudire et al. [143] developed a trajectory optimization method minimizing tracking errors in CNC machines that had unwanted vibration modes. The setpoints were parameterized using B-splines whose basis

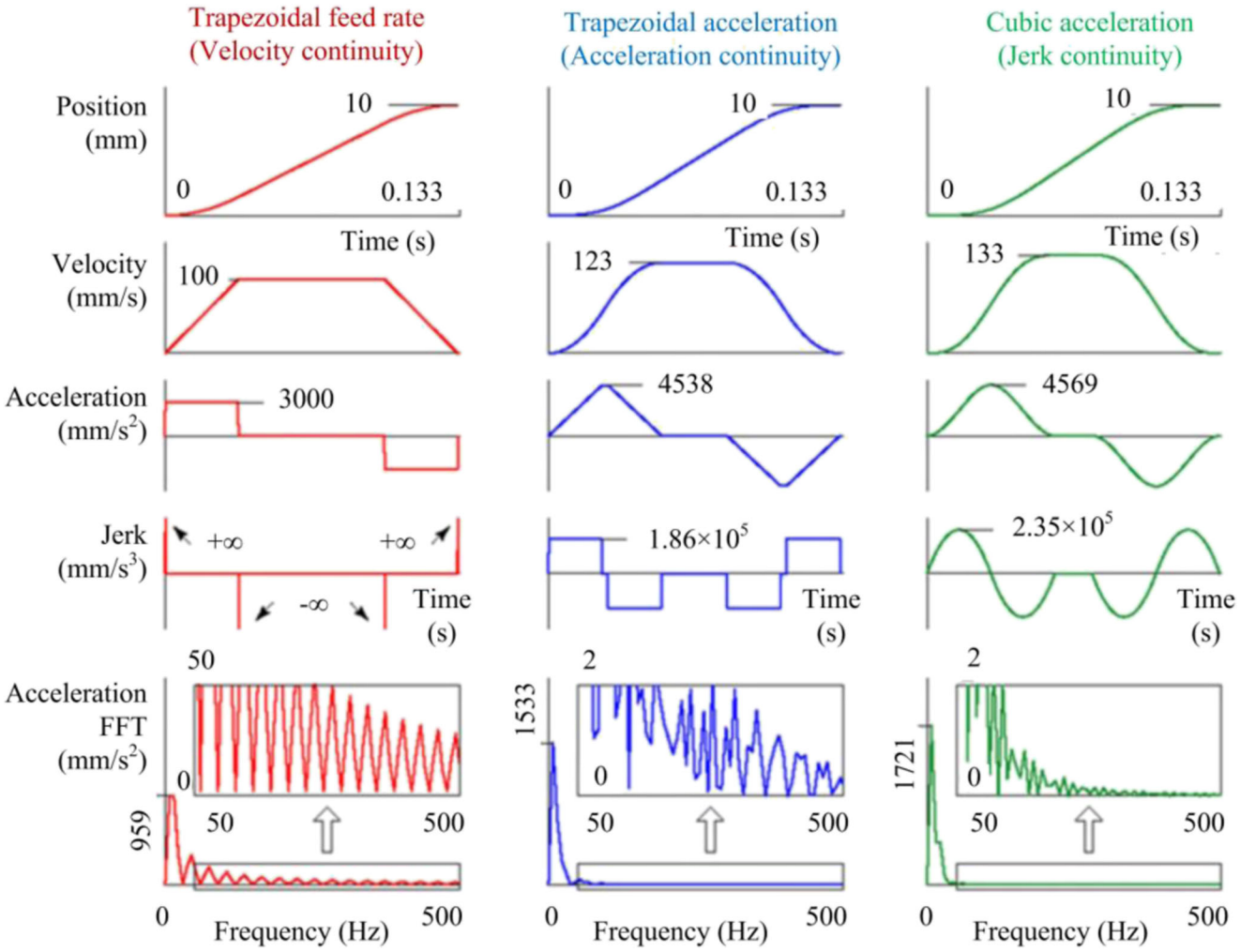

Fig. 17 Comparison of setpoints under three acceleration/deceleration strategies [16]

functions were filtered using a model of the machine's dynamics.

To sum up, for reducing the dynamic error, algorithms of tool path smoothing, setpoint profile smoothing, and setpoint filtering and shaping are used by CNC systems. Not only can these algorithms contribute to reduce tracking error (style 1 of dynamic error), but also they play an important role of suppressing the elastic deformation and vibration (styles 1 and 2 of dynamic error). The advanced CNC systems, such as FANUC 30i [144], SIEMENS 840D [145], and HEIDENHAIN iTNC530 [146], have been equipped with these functions.

Setpoint smoothing mentioned above is the technology of reducing the dynamic error through decreasing or limiting the feed rate, acceleration, and jerk, but sacrifices the machining efficiency [52, 147]. In order to further reduce the dynamic error with the same machining efficiency, the contour error [124, 148, 149] induced by the constraints of servo lag and the machine natural frequencies [130] have been taken into account in the interpolation.

5 Coordinating the dynamic errors

Trajectory error control is the basic task of multi-axis machine tools. When the dynamic errors of each axis are very small, the trajectory errors are considered to be very small. However, for the reasons listed in Sections 3 and 4, the dynamic errors of each axis or one axis cannot be effectively reduced to a small extent in some situations. At this point, coordinating dynamic error of individual axis is the choice for controlling the trajectory error.

5.1 Cross-coupling controller

Cross-coupling controller (CCC), developed by Koren [63], was first used to control the trajectory error of the two-axis linear trajectory.

CCC consists of two parts. One part is trajectory error estimation. The trajectory error is solved according to the geometric relation between tracking error and trajectory error [63, 150, 151]. The estimation method of trajectory error for a

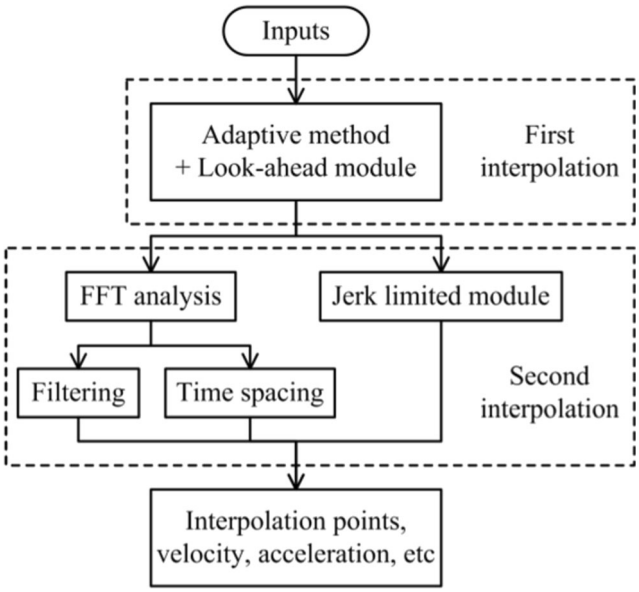

Fig. 18 NURBS parameter curve interpolation method with notch filter proposed by Liu et al. [130]

linear trajectory is relatively simple. The trajectory error is expressed as a function of tracking error and the slope of the linear trajectory. Figure 19 shows the trajectory error of the linear trajectory caused by tracking errors of two axes.

The trajectory error estimation methods for free form curves are relatively complex, which can be generally divided into two categories: local geometric approximations and iterative searches. The major problem of trajectory error estimation is that the approximation precision degrades in sharp corner regions [66, 152]. For example, the trajectory error estimation method of iterative searches suffers from the sudden change of trajectory error vector directions in regions of large curvature, which will lead to "lost corners" and cause sudden changes of acceleration in trajectory control. To combat this, Yang et al. [153] developed a computationally efficient nonparametric trajectory error estimation method for trajectory control. It first localized the large curvature regions and then modified the trajectory error vectors to sweep smoothly through the corner.

The other part of CCC is the control law of eliminating the trajectory error. The control law can be PID control, optimal control [154], adaptive control [155], fuzzy logic control [156], and robust control [157]. The structure of the CCC is shown in Fig. 20.

The CCC locates in the position loop. In order to ensure the control effect, the bandwidth of the CCC should be smaller than that of the position loop [158]. The frequency of trajectory error is generally very low, which can meet this requirement. Therefore, CCC can achieve good results in reducing trajectory error.

Due to the two rotary axes, the trajectory error estimation of the five-axis machine tool is more complicated. It was not until 2002 that Lo [159] reported five-axis CCC. His controller consisted of a real-time transformation between the machine tool coordinate and the workpiece coordinate. The tracking errors were firstly transformed to the workpiece coordinate for the estimation of trajectory error and the solving of control law. And then the control law was transformed to machine tool coordinate by inverse Jacobian matrix kinematics transformation, as shown in Fig. 21. The trajectory error estimation of the tool tip was obtained by the tangential projection along the tool path, and the trajectory error estimation of the tool orientation was calculated by the tracking errors of the two rotation axes.

Altintas and Sencer [160] established a method to estimate the trajectory error of a five-axis tool tip and a tool orientation trajectory error and realized the real-time compensation of the trajectory error by the sliding mode controller. Yang et al. established a kinematics model for five-axis machine tools with various structural types by using the spinor theory [161]. They improved the trajectory error estimation method [162], and then developed a trajectory error control method for five-axis machining based on model predictive control [163].

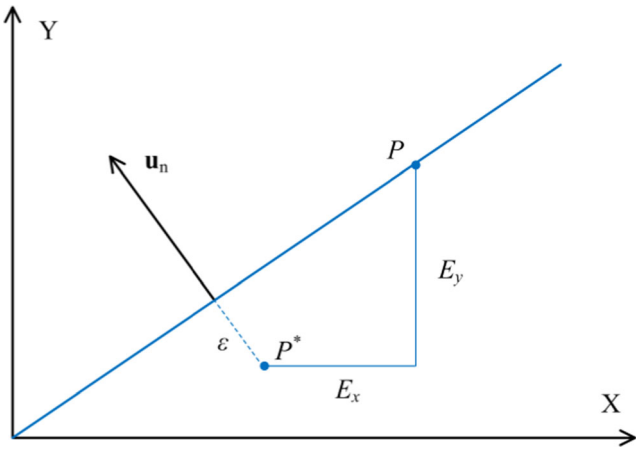

Fig. 19 Trajectory error of the linear trajectory caused by tracking errors of two axes [63]

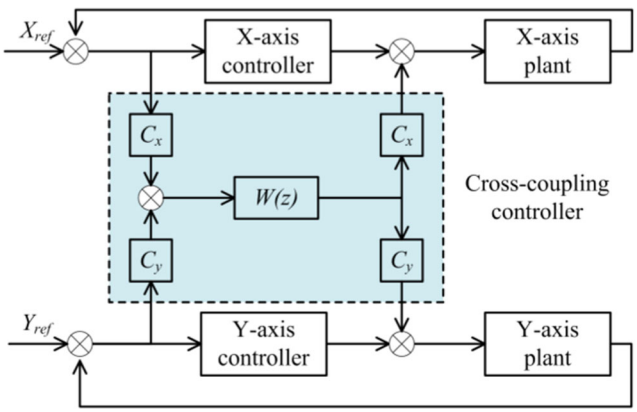

Fig. 20 Cross-coupling controller (CCC) [150]

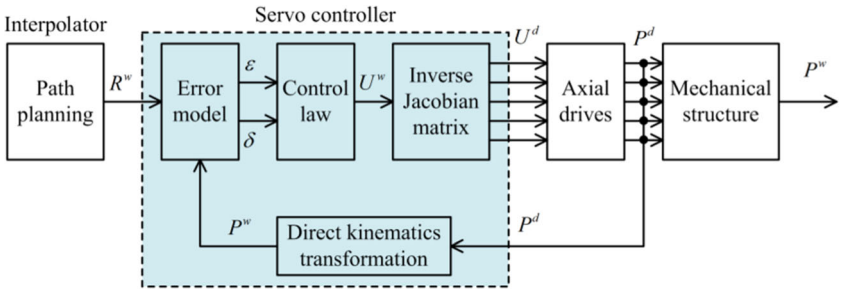

Fig. 21 The five-axis cross-coupling controller proposed by Lo [159]

Li et al. [164] proposed a double sliding mode contour control method, which could meet the requirements of reducing the trajectory error and meanwhile suppressing the mechanical vibration. Dong et al. [165] presented a five-axis CCC based on the double NURBS parametric interpolation algorithm. In a general way, trajectory error is estimated as the distance from the actual point to the line between each interpolation points. It neglects the error between the reference curve and interpolation line segment. To eliminate the influence on the accuracy of trajectory error estimation, Li et al. [166] constructed the Ferguson curve to approximate the reference curve between the interpolation points.

The CCC is a feedback control system based on online estimation of trajectory error. The control signal needs to be generated by the previous error signal. It is essentially a passive control method that produces trajectory error first and then adjusts/compensates it. To achieve lead control of trajectory error, Wang et al. [167] presented a trajectory error dynamical model-based position loop feedforward control strategy, which is completely different from the existing CCC.

In addition, the CCC uses the tracking error to estimate the trajectory error. Therefore, it can just compensate the trajectory error originating from the dynamic error of component 1.

5.2 Servo dynamics matching

Matching the servo dynamics of each axis, put forward by Poo et al. [168], was first used to analyze the trajectory error of linear trajectory. Xi et al. [169] further investigated the matching method of two-axis servo gain in circular trajectory machining.

For the five-axis machine tools, some specific methods were designed to explore the matching methods. Smith [70] identified the difference of servo bandwidth of each axis of the five-axis machine tool. A delay was added in the high bandwidth axis, so that it could be synchronized with the low bandwidth axis. Lei et al. identified the dynamic difference between rotary and rotary axes [170] and linear and rotary axes [171] in a five-axis machine tool by means of a ballbar. Through adjusting the position loop gains, the mismatch of servo dynamics between rotary and rotary axes and linear and rotary axes was eliminated. Later, Lei et al. [172] developed a universal test method by means of a ballbar which could inspect dynamic errors of all linear and rotary axes in a five-axis machine tool equipped with any type of CNC systems. Lin and Wu [173] stated that the mismatch of the servo dynamics between the linear axis and the rotary axis in the five-axis machine tool was the main reason for the machining error of the ISO10791-6 test trajectory. Wang et al. [174] and Jiang et al. [175] analyzed the trajectory error of the S-shaped piece. They also stated that the servo parameters affected the trajectory error. Duong et al. [176] presented an offline gain adjustment approach to reduce trajectory error in five-axis machining.

5.3 Tool path planning considering the dynamics mismatch

Tool paths directly affect the feed rate, acceleration, and jerk profiles assigned to each axis. Therefore, it directly affects the dynamic error of individual axis.

The classical methods of tool path planning, including iso-parametric, iso-planar, iso-scallop methods, etc., mainly focus on geometry accuracy by restraining scallop heights. In some new tool path planning methods, the influences of the tool path on cutting width [177–179], material removal rate [180, 181], and tool deformation [182] are further considered. However, the performance of machine tools, such as dynamic error, has not been considered in tool path planning.

Recently, Lu et al. [183] established the mathematical relationship between cutting direction, dynamics mismatch of feed axes, and trajectory error of a three-axis machine tool, as shown in Fig. 22. According to the dynamics mismatch of a three-axis machine tool, the optimal cutting directions could be determined for minimizing trajectory error. They verified that it is feasible in theory that the tool paths could be generated along the optimal cutting directions for reducing the trajectory error caused by dynamics mismatch between feed axes.

6 Conclusions

High-speed machining requires not only high feed rate, but also high feed acceleration and jerk. In sculptured surface machining, tool paths with large curvature change (such as

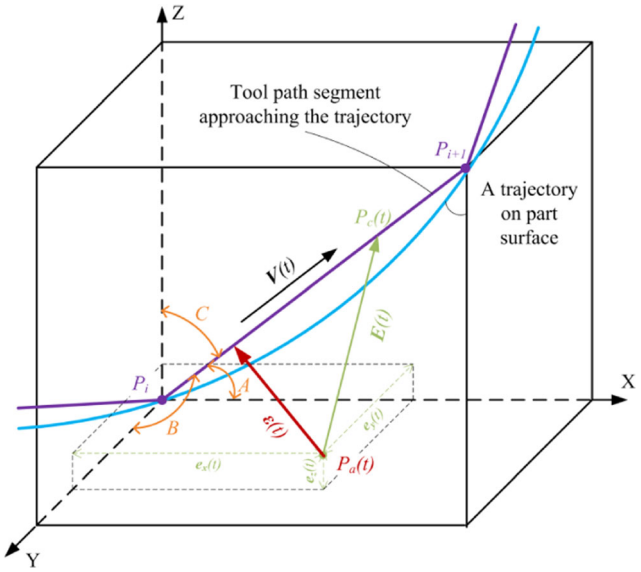

Fig. 22 The geometrical relationship between tracking errors, trajectory errors, and cutting directions established by Lu et al. [183]

sharp corner) increase the severity of feed rate change and further raise the requirement of feed acceleration and jerk. Under these situations, the dynamic error of machine tools often exceeds the geometric/thermo error, becoming the main reason that affects the machining error. Heretofore, although there are already many researches focused on the dynamic error, a systematic summary has not yet found in the literature. Therefore, in this review, the definition, components, and causes of dynamic error are summarized, and the research works on reducing the dynamic error are reviewed. Subsequently, some conclusions are drawn as follows:

1. The dynamic error is the deviation of actual displacement of effector end of axis relative to reference displacement during feed motion. The dynamic error presents two components according to the servo feed system itself and its input (setpoints): component 1 is the dynamic error inside the servo loop, which is mainly caused by the contradiction between the high bandwidth of setpoints and the low servo bandwidth of the servo feed system; component 2 is the dynamic error outside the servo loop, which originates from the elastic deformation and vibration of mechanical series outside the servo loop caused by the acceleration and jerk of setpoints.
2. From the point of view of the servo feed system itself, the basic strategies to reduce the dynamic error of individual axis are as follows: decreasing the phase lag and increasing the bandwidth of the servo feed system to reduce the dynamic error inside the servo loop (component 1); estimating or measuring the dynamic error of mechanical series outside the servo loop to compensate for the elastic deformation and suppress the vibration (component 2).
3. From the point of view of the servo feed system input (setpoints), the basic algorithms to reduce the dynamic error of individual axis are mainly the tool path smoothing, setpoint profile smoothing, and setpoint filtering and shaping. With these algorithms, the setpoints are more easily followed by the servo feed system, so that the dynamic error inside the servo loop can be obviously reduced (component 1). Meanwhile, the high frequencies in the setpoints which cause the elastic deformation and vibration are removed out, so that the dynamic error outside the servo loop can be suppressed (component 2).
4. Under the situation that the dynamic error of individual axis cannot be sufficiently reduced, coordinating the dynamic error of each axis is the basic strategy for reducing the trajectory dynamic error. These strategies mainly include the CCC, servo dynamics matching of each axis, and the tool path planning with the consideration of dynamics mismatch.

The feed acceleration in high-speed machining will be increased from 2 to 10 *g* [16]. The increase of acceleration will inevitably lead to the increase of the setpoint bandwidth and the increase of the high-frequency component. Meanwhile, for the servo feed system of especially five-axis machine tools, the servo bandwidth and control ability on mechanical deformation and vibration are difficult to improve due to the flexible links and high-order modes of mechanical structures [184]. Therefore, resolving the contradiction between the setpoints and the servo feed system is a great challenge for dynamic error in high-speed machining. There are still many researches that need to be carried out in the future:

1. The feedforward control, filtering, and sliding mode control have greatly improved the performance of the servo feed system. For higher servo bandwidth, future research will be aimed at the intelligent control strategies, such as enhanced learning [185] and data-driven control [186].
2. Compared with the dynamic error inside the servo loop (component 1), the dynamic error outside the servo loop (component 2) has not been solved very well. Therefore, the control strategies on the dynamic error outside the servo loop should be further developed and integrated into dynamic error inside the servo loop-oriented control strategies.
3. Although the investigations focused on the servo feed system itself and its input have been intensively carried out, these two parts are generally isolated from each other. These two parts need to be considered as a whole, so that the servo feed system of each axis can adapt to the differences and changes of the setpoints, and the differences in the servo dynamics of each axis can be considered in the setpoints.

Funding information This work is financially supported by the project of the National Natural Science Funds of China (Grant No. 51775421), the Major Project of High-end CNC Machine Tool and Basic Manufacturing Equipment of China (Grant No. 2015ZX04001002), the Major Project of High-end CNC Machine Tool and Basic Manufacturing Equipment of China (Grant No. 2016ZX04004-002-01), and the project funded by China Postdoctoral Science Foundation (Grant No. 2015 M570824).

References

1. Huo F, Poo A-N (2013) Precision contouring control of machine tools. Int J Adv Manuf Technol 64:319–333
2. Bohez ELJ (2002) Compensating for systematic errors in 5-axis NC machining. Comput Aided Des 34(5):391–403. https://doi.org/10.1016/S0010-4485(01)00111-7
3. Weekers WG, Schellekens PHJ (1995) Assessment of dynamic errors of CMMs for fast probing. CIRP Ann Manuf Technol 44(1):469–474
4. Ma J, Lu D, Zhao W (2015) Assembly errors analysis of linear axis of CNC machine tool considering component deformation. Int J Adv Manuf Technol 12:1–9
5. Li Y, Zhao W, Lan S, Ni J, Wu W, Lu B (2015) A review on spindle thermal error compensation in machine tools. Int J Mach Tool Manu 95:20–38
6. Sartori S, Zhang GX (1995) Geometric error measurement and compensation of machines. CIRP Ann 44(2):599–609. https://doi.org/10.1016/S0007-8506(07)60507-1
7. Ramesh R, Mannan MA, Poo AN (2000) Error compensation in machine tools—a review: part I: geometric, cutting-force induced and fixture-dependent errors. Int J Mach Tools Manuf 40(9):1235–1256. https://doi.org/10.1016/S0890-6955(00)00009-2
8. Schwenke H, Knapp W, Haitjema H, Weckenmann A, Schmitt R, Delbressine F (2008) Geometric error measurement and compensation of machines—an update. CIRP Ann 57(2):660–675. https://doi.org/10.1016/j.cirp.2008.09.008
9. Ibaraki S, Knapp W (2012) Indirect measurement of volumetric accuracy for three-axis and five-axis machine tools: a review. Int J Autom Technol 6(2):110–124
10. Ramesh R, Mannan MA, Poo AN (2000) Error compensation in machine tools—a review: part II: thermal errors. Int J Mach Tools Manuf 40(9):1257–1284. https://doi.org/10.1016/S0890-6955(00)00010-9
11. Uriarte L, Zatarain M, Axinte D, Yagüe-Fabra J, Ihlenfeldt S, Eguia J, Olarra A (2013) Machine tools for large parts. CIRP Ann 62(2):731–750. https://doi.org/10.1016/j.cirp.2013.05.009
12. Neugebauer R, Denkena B, Wegener K (2007) Mechatronic systems for machine tools. Ann CIRP 56(2):657–686
13. Schmitz TL, Ziegert JC, Canning JS, Zapata R (2008) Case study: a comparison of error sources in high-speed milling. Precis Eng 32:126–133
14. Kato N, Tsutsumi M, Sato R (2013) Analysis of circular trajectory equivalent to cone-frustum milling in five-axis machining centers using motion simulator. Int J Mach Tool Manu 64:1–11. https://doi.org/10.1016/j.ijmachtools.2012.07.013
15. Z-y J, Ma J-w, D-n S, Wang F-j, Liu W (2018) A review of contouring-error reduction method in multi-axis CNC machining. Int J Mach Tools Manuf 125:34–54. https://doi.org/10.1016/j.ijmachtools.2017.10.008
16. Altintas Y, Verl A, Brecher C, Uriarte L, Pritschow G (2011) Machine tool feed drives. CIRP Ann Manuf Technol 60:779–796
17. Koren Y, Lo CC (1992) Advanced controllers for feed drives. Annals of the CIRP 41(2):689–698
18. Koren Y (1997) Control of machine tools. J Manuf Sci Eng Trans ASME 119(11):749–755
19. Ramesh R, Mannan MA, Poo AN (2005) Tracking and contour error control in CNC servo systems. Int J Mach Tool Manu 45:301–326
20. Tang L, Landers RG (2013) Multiaxis contour control—the state of the art. IEEE Trans Control Syst Technol 21(6):1997–2010
21. Liang T, Lu D, Yang X, Zhang J, Ma X, Zhao W (2016) Feed fluctuation of ball screw feed systems and its effects on part surface quality. Int J Mach Tool Manu 101:1–9
22. Kamalzadeh A, Erkorkmaz K (2007) Accurate tracking controller design for high speed drives. Int J Mach Tool Manu 47(9):1393–1400
23. Yang XJ, Lu D, Zhang J, Zhao WH (2015) Investigation of the displacement fluctuation of the linear motor feed system considering the linear encoder vibration. Int J Mach Tool Manu 98:33–40
24. Mutilba U, Gomez-Acedo E, Kortaberria G, Olarra A, Yagüe-Fabra JA (2017) Traceability of on-machine tool measurement: a review. Sensors 17:1–38
25. Schmitz T, Ziegert J (1999) Examination of surface location error due to phasing of cutter vibrations. Precis Eng 23(1):51–62. https://doi.org/10.1016/S0141-6359(98)00025-7
26. Hu WX, Cao YL, Yang JX, Shang HC, Wang WB (2018) An error prediction model of NC machining process considering multiple error sources. Int J Adv Manuf Technol 94(5–8):1689–1698. https://doi.org/10.1007/s00170-016-9867-7
27. Chiu GTC, Yao B (1997) Adaptive robust contour tracking of machine tool feed drive systems—a task coordinate frame approach. Paper presented at the Proceedings of the American Control Conference, Albuquerque, New Mexico, June 1997
28. Huang XY, Zhao F, Mei XS, Tao Y, Tao T, Shi H, Liu X (2019) A novel triple-stage friction compensation for a feed system based on electromechanical characteristics. Precis Eng J Int Soc Precis Eng Nanotechnol 56:113–122. https://doi.org/10.1016/j.precisioneng.2018.11.006
29. Dong X, Okwudire CE (2018) An experimental investigation of the effects of the compliant joint method on feedback compensation of pre-sliding/pre-rolling friction. Precis Eng J Int Soc Precis Eng Nanotechnol 54:81–90. https://doi.org/10.1016/j.precisioneng.2018.05.004
30. Liu WR, Ren F, Sun YW, Jiang SL (2018) Contour error precompensation for three-axis machine tools by using cross-coupled dynamic friction control. Int J Adv Manuf Technol 98(1–4):551–563. https://doi.org/10.1007/s00170-018-2189-1
31. Lee W, Lee CY, Jeong YH, Min BK (2015) Friction compensation controller for load varying machine tool feed drive. Int J Mach Tool Manu 96:47–54. https://doi.org/10.1016/j.ijmachtools.2015.06.001
32. Yang X, Lu D, Zhang J, Zhao W (2016) Analysis on steady-state vibration induced by backlash in machine tool rotary table. Proc Inst Mech Eng C J Mech Eng Sci 231(22):4163–4171. https://doi.org/10.1177/0954406216662086
33. Shi S, Lin J, Wang X, Xu X (2015) Analysis of the transient backlash error in CNC machine tools with closed loops. Int J Mach Tools Manuf 93:49–60. https://doi.org/10.1016/j.ijmachtools.2015.03.009
34. Zhao W, Zhang J, Liu H, Yang X (2013) New evaluation method on the precision of NC machine tools. Eng Sci 15(1):93–98
35. Slamani M, Mayer R, Balazinski M, Zargarbashi SHH, Engin S, Lartigue C (2010) Dynamic and geometric error assessment of an XYC axis subset on five-axis high-speed machine tools using programmed end point constraint measurements. Int J Adv Manuf Technol 50:1063–1073
36. Slamani M, Mayer R, Balazinski M (2013) Concept for the integration of geometric and servo dynamic errors for predicting volumetric errors in five-axis high-speed machine tools: an application on a XYC three-axis motion trajectory using programmed end

point constraint measurements. Int J Adv Manuf Technol 65: 1669–1679
37. Zhong L, Bi Q, Huang N, Wang Y (2018) Dynamic accuracy evaluation for five-axis machine tools using S trajectory deviation based on R-test measurement. Int J Mach Tools Manuf 125:20–33
38. Heisel U, Gringel M (1996) Machine tool design requirements for high-speed machining. CIRP Ann 45(1):389–392. https://doi.org/10.1016/S0007-8506(07)63087-X
39. Kono D, Weikert S, Matsubara A, Yamazaki K (2012) Estimation of dynamic mechanical error for evaluation of machine tool structures. Int J Autom Technol 6(2):147–153
40. Barre P-J, Bearee R, Borne P, Dumetz E (2005) Influence of a jerk controlled movement law on the vibratory behaviour of high-dynamics systems. J Intell Robot Syst 42(3):275–293. https://doi.org/10.1007/s10846-004-4002-7
41. Lim H, Seo J-W, Choi C-H (2001) Torsional displacement compensation in position control for machining centers. Control Eng Pract 9(1):79–87. https://doi.org/10.1016/S0967-0661(00)00076-9
42. Zhu H, Fujimoto H (2015) Mechanical deformation analysis and high-precision control for ball-screw-driven stages. IEEE/ASME Trans Mechatron 20(2):956–966. https://doi.org/10.1109/TMECH.2014.2337933
43. Sugie T, Iwasaki T, Nakagawa H, Kohda S (1999) Compensation for the exponential type lost motion to improve the contouring accuracy of NC machine tools. Paper presented at the IECON'99. Conference Proceedings. 25th Annual Conference of the IEEE Industrial Electronics Society (Cat. No.99CH37029), 29 Nov.-3 Dec. 1999
44. Sugie T, Iwasaki T, Nakagawa T, Kohda T (2000) Compensation for position-varying lost motion to improve the contouring accuracy of NC machine tools. Paper presented at the 2000 26th Annual Conference of the IEEE Industrial Electronics Society. IECON 2000. 2000 IEEE International Conference on Industrial Electronics, Control and Instrumentation. 21st Century Technologies, 22–28 Oct. 2000
45. Kamalzadeh A, Gordon DJ, Erkorkmaz K (2010) Robust compensation of elastic deformations in ball screw drives. Int J Mach Tools Manuf 50(6):559–574. https://doi.org/10.1016/j.ijmachtools.2010.03.001
46. Huang H-W, Tsai M-S, Huang Y-C (2018) Modeling and elastic deformation compensation of flexural feed drive system. Int J Mach Tools Manuf 132:96–112. https://doi.org/10.1016/j.ijmachtools.2018.05.002
47. Wu N, Hu R, Sun Q (2004) Influence of rigidity of feed system with ball screw in NC lathe on positioning precision. Eng Sci 6(9): 46–49
48. Dong C, Zhang C, Wang B, Zhang G (2002) Prediction and compensation of dynamic errors for coordinate measuring machines. J Manuf Sci Eng Trans Asme 124(3):509–514
49. Weekers W (1996) Compensation for dynamic errors of coordinate measuring machines. Eindhoven University of Technology
50. Ahmadian MT, Vossoughi GR, Ramezani S (2007) Dynamic error analysis of gantry type coordinate measuring machines. Sci Iran 14(3):278–290
51. Bringmann B, Maglie P (2009) A method for direct evaluation of the dynamic 3D path accuracy of NC machine tools. CIRP Ann Manuf Technol 58:343–346
52. Parenti P, Albertelli P, Cau N, Bianchi G, Monno M (2011) A mechatronic study on a model-based compensation of inertial vibration in high speed machine tool. J Mach Eng 11(4):91–104
53. Knapp W, Weikert S (1999) Testing the contouring performance in 6 degrees of freedom. Ann CIRP 48:433–436
54. Ansoategui I, Campa FJ, López C, Díez M (2017) Influence of the machine tool compliance on the dynamic performance of the servo drives. Int J Adv Manuf Technol 90(9):2849–2861. https://doi.org/10.1007/s00170-016-9616-y
55. Thoma SM, Haas T, Nguyen H, Weikert S, Wegener K (2015) In- and cross-talk evaluation of different machine concepts. Paper presented at the 11th international conference and exhibition on laser metrology, coordinate measuring machine and machine tool performance, LAMDAMAP 2015, Huddersfield, UK, March 17–18, 2015
56. Nguyen MH, Weikert S, Wegener K (2012) Evaluation method of acceleration correlated position errors in machine tools. Br Med J 1(5):1327–1328
57. Zatarain M, Ruiz de Argandoña I, Illarramendi A, Azpeitia JL, Bueno R (2005) New control techniques based on state space observers for improving the precision and dynamic behaviour of machine tools. CIRP Ann 54(1):393–396. https://doi.org/10.1016/S0007-8506(07)60130-9
58. Mu YH, Ngoi BKA (1999) Dynamic error compensation of coordinate measuring machines for high-speed measurement. Int J Adv Manuf Technol 15:810–814
59. ISO (2009) Test code for machine tools. Part 8. Determination of vibration levels. ISO/DIS 230-8. Geneva
60. Andolfatto L, Lavernhe S, Mayer JRR (2011) Evaluation of servo, geometric and dynamic error sources on five-axis high-speed machine tool. Int J Mach Tool Manu 51:787–796
61. Kono D, Matsubara A, Nagaoka K, Yamazaki K (2012) Analysis method for investigating the influence of mechanical components on dynamic mechanical error of machine tools. Precis Eng 36(3): 477–484. https://doi.org/10.1016/j.precisioneng.2012.02.006
62. Pritschow G (1996) On the influence of the velocity gain factor on the path deviation. CIRP Ann 45(1):367–371. https://doi.org/10.1016/S0007-8506(07)63082-0
63. Koren Y (1980) Cross-coupled biaxial computer control for manufacturing systems. ASME Trans J Dyn Syst Meas Control 102:265–272
64. Tomizuka M (1987) Zero phase error tracking algorithm for digital control. ASME Trans J Dyn Syst Meas Control 109(1):65–68
65. Funahashi Y, Yamada M (1993) Zero phase error tracking controllers with optimal gain characteristics. J Dyn Syst Meas Control Trans Asme 115(3):311–318
66. Rahaman M, Seethaler R, Yellowley I (2015) A new approach to contour error control in high speed machining. Int J Mach Tool Manu 88:42–50
67. Li XW, Zhang J, Zhao WH, Lu BH (2016) A zero phase error tracking based path pre-compensation method for high speed machining. J Mech Eng Sci 230(2):230–239
68. Chen X, Liu C, Zhou N, Wang B (2014) Controller design based on ZPETC-FF and DOB for precision motion platform. J Harbin Inst Technol 46(1):1–6
69. Wang L, Li X (2014) Zero phase adaptive robust control of direct drive XY table. J Shenyang Univ Technol 36(2):121–126
70. Smith DA (1999) Wide bandwidth control of high-speed milling machine feed drives. University of Florida
71. Chen YC, Tlusty J (1995) Effect of low friction guideways and leadscrew flexibility on dynamics of high-speed machines. CIRP Ann Manuf Technol 44(1):353–356
72. Erkorkmaz K, Kamalzadeh A (2007) Compensation of axial vibrations in ball screw drives. CIRP Ann Manuf Technol 56(1): 373–378
73. Erkorkmaz K, Kamalzadeh A (2006) High bandwidth control of ball screw drives. CIRP Ann Manuf Technol 55(1):393–398
74. Altintas Y, Erkorkmaz K, Zhu WH (2000) Sliding mode controller design for high speed feed drives. CIRP Ann Manuf Technol 49: 265–270
75. Okwudire C, Altintas Y (2009) Minimum tracking error control of flexible ball screw drives using a discrete-time sliding mode controller. ASME Trans J Dyn Syst Meas Control 131:051006

76. Pritschow G, Croon N (2013) Ball screw drives with enhanced bandwidth by modification of the axial bearing. CIRP Ann Manuf Technol 62:383–386
77. Verl A, Frey S (2012) Improvement of feed drive dynamics by means of semi-active damping. CIRP Ann Manuf Technol 61(1): 351–354
78. Sun Z, Pritschow G, Lechler A (2016) Enhancement of feed drive dynamics using additional table speed feedback. CIRP Ann Manuf Technol 65(1):357–360
79. Sun Z, Zahn P, Verl A, Lechler A (2017) A new control principle to increase the bandwidth of feed drives with large inertia ratio. Int J Adv Manuf Technol 91:1747–1752
80. Sun Z, Pritschow G, Zahn P, Lechler A (2018) A novel cascade control principle for feed drives of machine tools. CIRP Ann Manuf Technol
81. Sencer B, Dumanli A (2017) Optimal control of flexible drives with load side feedback. CIRP Ann Manuf Technol 66(1):357–360
82. Liu H, Zhang J, Zhao W (2017) An intelligent non-collocated control strategy for ball-screw feed drives with dynamic variations. Engineering 3:107
83. Dumanli A, Sencer B (2018) Optimal high-bandwidth control of ball-screw drives with acceleration and jerk feedback. Precis Eng J Int Soc Precis Eng Nanotechnol 54:254–268. https://doi.org/10.1016/j.precisioneng.2018.06.002
84. FANUC FANUC AC Servo Motor αi series, FANUC AC Servo Motor βi series, FANUC Linear Motor LiS series, FANUC Synchronous Built-In Servo Motor DiS series parameter manual. B-65270EN/07 edn.
85. HEIDENHAIN (2013) Dynamic precision—machining dynamically and with high accuracy
86. van Loon SJLM, Hunnekens BGB, Simon AS, van de Wouw N, Heemels WPMH (2018) Bandwidth-on-demand motion control. IEEE Trans Control Syst Technol 26(1):265–273
87. Wang L, Liu H, Yang L, Zhang J, Zhao W, Lu B (2015) The effect of axis coupling on machine tool dynamics determined by tool deviation. Int J Mach Tool Manu 88:71–81
88. Matsubara A, Nagaoka K, Fujita T (2011) Model-reference feedforward controller design for high-accuracy contouring control of machine tool axes. CIRP Ann 60(1):415–418. https://doi.org/10.1016/j.cirp.2011.03.029
89. Denkena B, Overmeyer L, Litwinski KM, Peters R (2014) Compensation of geometrical deviations via model based-observers. Int J Adv Manuf Technol 73(5):989–998. https://doi.org/10.1007/s00170-014-5885-5
90. Weikert S (2004) R-test, a new device for accuracy measurements on five axis machine tools. CIRP Ann 53(1):429–432. https://doi.org/10.1016/S0007-8506(07)60732-X
91. Steinlin M, Weikert S, Wegener K (2010) Open loop inertial cross-talk compensation based on measurement data. Paper presented at the 25th annual meeting of the American Society for Precision Engineering, ASPE 2010, Atlanta, GA, United States, October 31, 2010 - November 4, 2010
92. Keck A, Sawodny O, Gronle M, Haist T, Osten W (2018) Model-based compensation of dynamic errors in measuring machines and machine tools. IEEE ASME Trans Mechatron 23(5):2252–2262. https://doi.org/10.1109/tmech.2018.2868012
93. Bosetti P, Bertolazzi E (2014) Feed-rate and trajectory optimization for CNC machine tools. Robot Comput Integr Manuf 30(6): 667–677. https://doi.org/10.1016/j.rcim.2014.03.009
94. Dong J, Ferreira PM, Stori JA (2007) Feed-rate optimization with jerk constraints for generating minimum-time trajectories. Int J Mach Tools Manuf 47(12):1941–1955. https://doi.org/10.1016/j.ijmachtools.2007.03.006
95. Weck M, Ye G (1990) Sharp corner tracking using the IKF control strategy. CIRP Ann Manuf Technol 39(1):473–441
96. Yang DCH, Kong T (1994) Parametric interpolator versus linear interpolator for precision CNC machining. Comput Aided Des 26(3):225–234. https://doi.org/10.1016/0010-4485(94)90045-0
97. Shpitalni M, Koren Y, Lo CC (1994) Realtime curve interpolators. Comput Aided Des 26(11):832–838
98. Erkorkmaz K, Altintas Y (2001) High speed CNC system design. Part I: jerk limited trajectory generation and quintic spline interpolation. Int J Mach Tools Manuf 41(9):1323–1345. https://doi.org/10.1016/S0890-6955(01)00002-5
99. Timar SD, Farouki RT (2008) Time-optimal traversal of curved paths by Cartesian CNC machines under both constant and speed-dependent axis acceleration bounds. Robot Comput Integr Manuf 24(1):16–31. https://doi.org/10.1016/j.rcim.2006.06.002
100. Bedi S (1993) Advanced interpolation techniques for N.C. machines. J Manuf Sci Eng 115(3):329. https://doi.org/10.1115/1.2901668
101. Sata T, Kimura F, Okada N, Hosaka M (1981) A new method of NC interpolation for machining the sculptured surface. CIRP Ann 30(1):369–372. https://doi.org/10.1016/S0007-8506(07)60959-7
102. Wang YS, Yang DS, Liu YZ (2014) A real-time look ahead interpolation algorithm based on Akima curve fitting. Int J Mach Tool Manu 85:122–130
103. Wang JB, Yau HT (2014) Universal real-time NURBS interpolator on a PC-based controller. J Adv Manuf Technol 71(4):497–507
104. Cheng MY, Tsai MC, Kuo JC (2002) Real-time NURBS command generators for CNC servo controllers. Int J Mach Tools Manuf 42(7):801–813. https://doi.org/10.1016/S0890-6955(02)00015-9
105. Lai J-Y, Lin K-Y, Tseng S-J, Ueng W-D (2008) On the development of a parametric interpolator with confined chord error, feedrate, acceleration and jerk. Int J Adv Manuf Technol 37(1): 104–121. https://doi.org/10.1007/s00170-007-0954-7
106. Zhong WB, Luo XC, Chang WL, Ding F, Cai YK (2018) A real-time interpolator for parametric curves. Int J Mach Tool Manu 125:133–145. https://doi.org/10.1016/j.ijmachtools.2017.11.010
107. Lin MT, Lee MC, Lee JC, Lee CY, Jian ZW (2016) A look-ahead interpolator with curve fitting algorithm for five-axis tool path. Paper presented at the 2016 IEEE international conference on advanced intelligent mechatronics, Banff, Alberta, Canada, July 12-15, 2016
108. Shi J, Bi QZ, Zhu LM, Wang YH (2015) Corner rounding of linear five-axis tool path by dual PH curves blending. Int J Mach Tool Manu 88:223–236
109. Beudaert X, Pechard P-Y, Tournier C (2011) 5-Axis tool path smoothing based on drive constraints. Int J Mach Tools Manuf 51(12):958–965. https://doi.org/10.1016/j.ijmachtools.2011.08.014
110. Tulsyan S, Altintas Y (2015) Local toolpath smoothing for five-axis machine tools. Int J Mach Tools Manuf 96:15–26. https://doi.org/10.1016/j.ijmachtools.2015.04.014
111. Sencer B, Shamoto E (2014) Curvature-continuous sharp corner smoothing scheme for Cartesian motion systems. Paper presented at the 2014 IEEE 13th international workshop on advanced motion control (AMC), 14–16 March 2014
112. Sencer B, Ishizaki K, Shamoto E (2015) A curvature optimal sharp corner smoothing algorithm for high-speed feed motion generation of NC systems along linear tool paths. Int J Adv Manuf Technol 76(9):1977–1992. https://doi.org/10.1007/s00170-014-6386-2
113. Zhao H, Zhu L, Ding H (2013) A real-time look-ahead interpolation methodology with curvature-continuous B-spline transition scheme for CNC machining of short line segments. Int J Mach Tool Manu 65:88–98
114. Hu Q, Chen YP, Jin XL, Yang JX (2019) A real-time C-3 continuous local corner smoothing and interpolation algorithm for CNC

machine tools. J Manuf Sci Eng Trans ASME 141(4):16. https://doi.org/10.1115/1.4042606
115. Tajima S, Sencer B (2017) Global tool-path smoothing for CNC machine tools with uninterrupted acceleration. Int J Mach Tools Manuf 121:81–95. https://doi.org/10.1016/j.ijmachtools.2017.03.002
116. Beudaert X, Lavernhe S, Tournier C (2013) 5-Axis local corner rounding of linear tool path discontinuities. Int J Mach Tools Manuf 73:9–16. https://doi.org/10.1016/j.ijmachtools.2013.05.008
117. Tajima S, Sencer B (2019) Accurate real-time interpolation of 5-axis tool-paths with local corner smoothing. Int J Mach Tool Manu 142:1–15. https://doi.org/10.1016/j.ijmachtools.2019.04.005
118. Zhou J, Sun Y, Guo D (2014) Adaptive feedrate interpolation with multiconstraints for five-axis parametric toolpath. Int J Adv Manuf Technol 71(9):1873–1882. https://doi.org/10.1007/s00170-014-5635-8
119. Jia Z, Wang L, Ma J, Zhao K, Liu W (2014) Feed speed scheduling method for parts with rapidly varied geometric feature based on drive constraint of NC machine tool, vol 87. https://doi.org/10.1016/j.ijmachtools.2014.07.010
120. Yeh SS, Hsu PL (1999) The speed-controlled interpolator for machining parametric curves. Comput Aided Des 31(5):349–357. https://doi.org/10.1016/S0010-4485(99)00035-4
121. Liu M, Huang Y, Yin L, Guo J, Shao X, Zhang G (2014) Development and implementation of a NURBS interpolator with smooth feedrate scheduling for CNC machine tools. Int J Mach Tools Manuf 87:1–15. https://doi.org/10.1016/j.ijmachtools.2014.07.002
122. Yeh S-S, Hsu P-L (2002) Adaptive-feedrate interpolation for parametric curves with a confined chord error. Comput Aided Des 34(3):229–237. https://doi.org/10.1016/S0010-4485(01)00082-3
123. Zhiming X, Jincheng C, Zhengjin F (2002) Performance evaluation of a real-time interpolation algorithm for NURBS curves. Int J Adv Manuf Technol 20(4):270–276. https://doi.org/10.1007/s001700200152
124. Jia Z-Y, Song D-N, Ma J-W, Hu G-Q, Su W-W (2017) A NURBS interpolator with constant speed at feedrate-sensitive regions under drive and contour-error constraints. Int J Mach Tools Manuf 116:1–17. https://doi.org/10.1016/j.ijmachtools.2016.12.007
125. Sun YW, Bao YR, Kang KX, Guo DM (2013) An adaptive feedrate scheduling method of dual NURBS curve interpolator for precision five axis CNC machining. Int J Adv Manuf Technol 68:1977–1987
126. Erkorkmaz K, Chen Q-G, Zhao M-Y, Beudaert X, Gao X-S (2017) Linear programming and windowing based feedrate optimization for spline toolpaths. CIRP Ann 66(1):393–396. https://doi.org/10.1016/j.cirp.2017.04.058
127. Jin YA, He Y, Fu JZ (2013) A look-ahead and adaptive speed control algorithm for parametric interpolation. Int J Adv Manuf Technol 69:2613–2620
128. Beudaert X, Lavernhe S, Tournier C (2012) Feedrate interpolation with axis jerk constraints on 5-axis NURBS and G1 tool path. Int J Mach Tools Manuf 57:73–82. https://doi.org/10.1016/j.ijmachtools.2012.02.005
129. Qiao ZF, Wang HH, Liu ZZ, Wang TY, Hu M (2015) Nanoscale trajectory planning with flexible Acc/Dec and look-ahead method. Int J Adv Manuf Technol 96:94–105
130. Liu X, Ahmad F, Yamazaki K, Mori M (2005) Adaptive interpolation scheme for NURBS curves with the integration of machining dynamics. Int J Mach Tools Manuf 45(4):433–444. https://doi.org/10.1016/j.ijmachtools.2004.09.009
131. Feng J, Li Y, Wang Y, Chen M (2010) Design of a real-time adaptive NURBS interpolator with axis acceleration limit. Int J Adv Manuf Technol 48(1):227–241. https://doi.org/10.1007/s00170-009-2261-y
132. Nam S-H, Yang M-Y (2004) A study on a generalized parametric interpolator with real-time jerk-limited acceleration. Comput Aided Des 36(1):27–36. https://doi.org/10.1016/S0010-4485(03)00066-6
133. Wang YS, Yang DS, Gai RL, Wang SH, Sun SJ (2015) Design of trigonometric velocity scheduling algorithm based on pre-interpolation and look-ahead interpolation. Int J Mach Tool Manu 96:94–105
134. Shahzadeh A, Khosravi A, Robinette T, Nahavandi S (2018) Smooth path planning using biclothoid fillets for high speed CNC machines. Int J Mach Tool Manu 132:36–49. https://doi.org/10.1016/j.ijmachtools.2018.04.003
135. Tajima S, Sencer B, Shamoto E (2018) Accurate interpolation of machining tool-paths based on FIR filtering. Precis Eng-J Int Soc Precis Eng Nanotechnol 52:332–344. https://doi.org/10.1016/j.precisioneng.2018.01.016
136. Sencer B, Tajima S (2017) Frequency optimal feed motion planning in computer numerical controlled machine tools for vibration avoidance. J Manuf Sci Eng Trans ASME 139(1):13. https://doi.org/10.1115/1.4034140
137. Sencer B, Dumanli A, Yamada Y (2018) Spline interpolation with optimal frequency spectrum for vibration avoidance. CIRP Ann Manuf Technol 67(1):377–380. https://doi.org/10.1016/j.cirp.2018.03.002
138. Mansour SZ, Seethaler R (2017) Feedrate optimization for computer numerically controlled machine tools using modeled and measured process constraints. J Manuf Sci Eng Trans ASME 139(1):9. https://doi.org/10.1115/1.4033933
139. Singer NC, Seering WP (1990) Preshaping command inputs to reduce system vibration. J Dyn Syst Meas Control Trans ASME 112(1):76–82
140. Dietmair A, Verl A (2009) Drive based vibration reduction for production machines. Mod Mach Sci J 3:130–134
141. Altintas Y, Khoshdarregi MR (2012) Contour error control of CNC machine tools with vibration avoidance. CIRP Ann Manuf Technol 61:335–338
142. Jones SD, Ulsoy AG (1999) An approach to control input shaping with application to coordinate measuring machines. J Dyn Syst Meas Control 121(2):242–247. https://doi.org/10.1115/1.2802461
143. Okwudire C, Ramani K, Duan M (2016) A trajectory optimization method for improved tracking of motion commands using CNC machines that experience unwanted vibration. CIRP Ann Manuf Technol 65(1):373–376. https://doi.org/10.1016/j.cirp.2016.04.100
144. AI Nano CNC for high-speed high-accuracy machining, FANUC series 31i/32i/30i/35i-Model B, FANUC series 31i-Model B5-datasheet (2004). FANUC Corporation
145. Milling with SIMUMERIK: mold making with 3- to 5-axis simultaneous milling manual (2013) Siemens Corporation
146. iTNC 530 HSCI NC Software 606 420-02, 606 421-02-technique manual (2012) Heidenhain Corporation
147. Flores V, Ortega C, Alberti M, Rodriguez CA, de Ciurana J, Elias A (2007) Evaluation and modeling of productivity and dynamic capability in high-speed machining centers. Int J Adv Manuf Technol 33(3–4):403–411. https://doi.org/10.1007/s00170-006-0784-z
148. Dong J, Wang T, Li B, Ding Y (2014) Smooth feedrate planning for continuous short line tool path with contour error constraint. Int J Mach Tools Manuf 76:1–12. https://doi.org/10.1016/j.ijmachtools.2013.09.009
149. Lin M-T, Tsai M-S, Yau H-T (2007) Development of a dynamics-based NURBS interpolator with real-time look-ahead algorithm. Int J Mach Tools Manuf 47(15):2246–2262. https://doi.org/10.1016/j.ijmachtools.2007.06.005
150. Koren Y, Lo CC (1991) Variable-gain cross-coupling controller for contouring. CIRP Ann Manuf Technol 40(1):371–374

151. Shih Y-T, Chen C-S, Lee A-C (2002) A novel cross-coupling control design for Bi-axis motion. Int J Mach Tool Manu 42: 1539–1548
152. Wang Z, Hu CX, Zhu Y, He SQ, Zhang M, Mu HH (2018) Newton-ILC contouring error estimation and coordinated motion control for precision multiaxis systems with comparative experiments. IEEE Trans Ind Electron 65(2):1470–1480. https://doi.org/10.1109/tie.2017.2733455
153. Yang X, Seethaler R, Zhan CP, Lu D, Zhao WH (2019) A novel contouring error estimation method or contouring control. IEEE-ASME Trans Mechatron 24(4):1902–1907. https://doi.org/10.1109/tmech.2019.2928791
154. Kulkarni PK, Srinivasan K (1989) Optimal contouring control of multi-axial feed drive servomechanisms. J Dyn Syst Meas Control Trans ASME 111:140–147
155. Chung HY, Liu CH (1992) A model-referenced adaptive control strategy for improving contour accuracy of multiaxis machine tools. IEEE Trans Ind Appl 28:221–227
156. Yeh ZM (1998) A cross-coupled bistage fuzzy logic controller for biaxis servomechanism control. Fuzzy Sets Syst 97:265–275
157. Yeh SS, Hsu PL (1999) Theory and applications of the robust crosscoupled control design. ASME J Dyn Syst Meas Control 121:524–530
158. Srinivasan K, Kulkarni PK (1990) Cross-coupled control of biaxial feed drive servomechanisms. J Dyn Syst Meas Control Trans ASME 112(2):225–232
159. Lo CC (2002) A tool-path control scheme for five-axis machine tools. Int J Mach Tools Manuf 42:79–88
160. Altintas Y, Sencer B (2010) High speed contouring control strategy for five-axis machine tools. CIRP Ann Manuf Technol 59(1): 417–420
161. Yang JX, Altintas Y (2013) Generalized kinematics of five-axis serial machines with non-singular tools path generation. Int J Mach Tool Manu 75:119–132
162. Yang JX, Altintas Y (2015) A generalized on-line estimation and control of five-axis contouring errors of CNC machine tools. Int J Mach Tool Manu 88:9–23
163. Yang JX, Zhang HT, Ding H (2017) Contouring error control of the tool center point function for five axis machine tools based on model predictive control. Int J Adv Manuf Technol 88:2909–2919
164. Li XF, Zhao H, Zhao X, Ding H (2016) Dual sliding mode contouring control with high accuracy contour error estimation for five-axis CNC machine tools. Int J Mach Tool Manu 108: 74–82
165. Dong B, Liu Y, Wang Z (2014) Study on 5-axis CNC system cross-coupled controller based on double NURBS hybrid parametric interpolation algorithm. China Mech Eng 25(22):3038–3044
166. Pi SW, Liu Q, Liu QT (2018) A novel dynamic contour error estimation and control in high-speed CNC. Int J Adv Manuf Technol 96(1–4):547–560. https://doi.org/10.1007/s00170-018-1629-2
167. Wang Z, Hu CX, Zhu Y (2019) Dynamical model based contouring error position-loop feedforward control for multiaxis motion systems. IEEE Trans Ind Inform 15(8):4686–4695. https://doi.org/10.1109/tii.2019.2895071
168. Poo AN, Bollinger JG, Younkin GW (1972) Dynamic errors in type 1 contouring systems. IEEE Trans Ind Appl IA-8(4):477–484
169. Xi XC, Poo AN, Hong GS (2009) Improving contouring accuracy by tuning gains for a bi-axial CNC machine. Int J Mach Tool Manu 49:395–460
170. Lei WT, Sung MP, Liu WL, Chuang YC (2007) Double ballbar test for the rotary axes of five-axis CNC machine tools. Int J Mach Tools Manuf 47(2):273–285. https://doi.org/10.1016/j.ijmachtools.2006.03.012
171. Lei WT, Paung IM, Yu CC (2009) Total ballbar dynamic tests for five axis CNC machine tools. Int J Mach Tool Manu 49:488–499
172. Lei W-T, Wang W-C, Fang T-C (2014) Ballbar dynamic tests for rotary axes of five-axis CNC machine tools. Int J Mach Tools Manuf 82–83:29–41. https://doi.org/10.1016/j.ijmachtools.2014.03.008
173. Lin MT, Wu SK (2013) Modeling and analysis of servo dynamics errors on measuring paths of five axis machine tools. Int J Mach Tool Manu 66:1–14
174. Wang W, Zhang X, Zheng C, Zhao X, Bian Z, Jiang Z (2014) Analysis for machining precision prediction and influencing factors of complex surface in aviation. J Univ Electron Sci Technol China 43(5):787–793
175. Jiang Z, Ding JX, Song ZY (2016) Modeling and simulation of surface morphology abnormality of S test piece machined by five axis CNC machine tool. Int J Adv Manuf Technol 85:2745–2759
176. Duong TQ, Rodriguez-Ayerbe P, Lavernhe S, Tournier C, Dumur D (2019) Contour error pre-compensation for five-axis high speed machining: offline gain adjustment approach. Int J Adv Manuf Technol 100(9–12):3113–3125. https://doi.org/10.1007/s00170-018-2859-z
177. Marciniak K (1987) Influence of surface shape on admissible tool positions in 5-aixs face milling. Comput Aided Des 19(5):233–236
178. Kruth JP, Klewais P (1994) Optimization and dynamic adaptation of the cutter inclination during five-axis milling of sculptured surfaces. CIRP Ann Manuf Technol 43(1):443–448
179. Chiou CJ, Lee YS (2002) A machining potential field approach to tool path generation for multi-axis sculptured surface machining. Comput Aided Des 34(5):357–371
180. Kim T, Sarma SE (2002) Tool path generation along directions of maximum kinematic performance; a first cut at machine-optimal paths. Comput Aided Des 34(6):453–468
181. Giri V, Bezbaruah D, Bubna P, Choudhury AR (2005) Selection of master cutter paths in sculptured surface machining by employing curvature principle. Int J Mach Tool Manu 45(10):1202–1209
182. Lim EM, Menq CH (1997) Integrated planning for precision machining of complex surfaces. Part 1: cutting-path and feedrate optimization. Int J Mach Tool Manu 37(1):61–75
183. Lu D, Liu S, Li X, Wu D, Zhao W, Lu B (2017) Optimal cutting directions by considering the dynamic mismatch between feed axes of machine tools. Int J Adv Manuf Technol 95:1607–1615. https://doi.org/10.1007/s00170-017-1243-8
184. Yuen A, Altintas Y (2016) Trajectory generation and control of a 9 axis CNC micromachining center. CIRP Ann Manuf Technol 65: 349–352
185. Fernandez-Gauna B, Ansoategui I, Etxeberria-Agiriano I, Graña M (2014) Reinforcement learning of ball screw feed drive controllers. Eng Appl Artif Intell 30:107–117
186. Hou ZS, Wang Z (2013) From model-based control to data-driven control: survey, classification and perspective. Inf Sci 235:3–35